Combined unitary and symmetric group approach applied to low-dimensional Heisenberg spin systems

(article starts on next page)

Combined unitary and symmetric group approach applied to low-dimensional Heisenberg spin systems

Werner Dobrautz [1,2,*] Vamshi M. Katukuri [1] Nikolay A. Bogdanov [1] Daniel Kats [1] Giovanni Li Manni [1] and Ali Alavi [1,3]

[1]*Max Planck Institute for Solid State Research, Heisenbergstr. 1, 70569 Stuttgart, Germany*
[2]*Department of Chemistry and Chemical Engineering, Chalmers University of Technology, 41296 Gothenburg, Sweden*
[3]*Yusuf Hamied Department of Chemistry, University of Cambridge, Lensfield Road, Cambridge CB2 1EW, United Kingdom*

A novel combined unitary and symmetric group approach is used to study the spin-$\frac{1}{2}$ Heisenberg model and related Fermionic systems in a total spin-adapted representation, using a linearly-parameterised Ansatz for the many-body wave function. We show that a more compact ground-state wave function representation—indicated by a larger leading ground-state coefficient—is obtained when combining the symmetric group $\mathcal{S}_n$, in the form of permutations of the underlying lattice site ordering, with the cumulative spin coupling based on the unitary group $\mathrm{U}(n)$. In one-dimensional systems the observed compression of the wave function is reminiscent of block-spin renormalization group approaches, and allows us to study larger lattices (here taken up to 80 sites) with the spin-adapted full configuration interaction quantum Monte Carlo method, which benefits from the sparsity of the Hamiltonian matrix and the corresponding sampled eigenstates that emerge from the reordering. We find that in an optimal lattice ordering the configuration state function with highest weight already captures with high accuracy the spin-spin correlation function of the exact ground-state wave function. This feature is found for more general lattice models, such as the Hubbard model, and *ab initio* quantum chemical models, exemplified by one-dimensional hydrogen chains. We also provide numerical evidence that the optimal lattice ordering for the unitary group approach is not generally equivalent to the optimal ordering obtained for methods based on matrix-product states, such as the density-matrix renormalization group approach.

I. INTRODUCTION

Symmetry is a concept of paramount importance in physics and chemistry. Continuous symmetry transformations are related to conservation laws by Noether's theorem [1] and are represented by Lie groups [2], while discrete symmetry transformations, given by an operator $\hat{T}$ that commutes with the Hamiltonian $\hat{H}$ of a system, are of special importance in electronic structure calculations. Since a set of commuting operators can be simultaneously diagonalized, utilizing the eigenfunctions $|\Phi\rangle$ of the operator $\hat{T}$ causes $\hat{H}$ to have a block-diagonal structure in this basis. Common discrete symmetries used in electronic structure calculations are the discrete translational symmetry on a lattice (by the use of a momentum space basis/Bloch functions [3]), the point-group symmetries of lattices and molecules (by the use of symmetry-adapted molecular orbitals) or conservation of the number of electron n_{el} and the projection of the total spin (magnetization) $\hat{S}_z$ [by the use of a Slater-determinant (SD) or

"spin"-basis ($|\uparrow\downarrow\ldots\rangle$) with fixed n_{el} and m_s]. More elaborate symmetries, such as the global SU(2) spin-rotation symmetry of spin-preserving nonrelativistic Hamiltonians, necessitate a more elaborate consideration, with the unitary group approach (UGA) [4–7] being a notable example.

The fundamental principle of quantum mechanics, which states that no observable physical quantity must change after exchanging two indistinguishable particles, leads to the concept of exchange or permutation symmetry. The finite symmetric group $\mathcal{S}_n$ consists of all $n!$ possible permutations of n objects and, following the spin-statistics theorem [8], fermionic wave functions must transform as the antisymmetric irreducible representation of $\mathcal{S}_n$. Additionally, Caley's theorem states that every group, and thus symmetry, can be realized as a subgroup of a symmetric group [9].

In addition to the exchange of *particle* labels, we can also consider the effect of exchanging *orbital* or *lattice-site* labels. An exchange of a pair of orbitals can be seen as a 180° rotation between the two orbitals, a particularly simple unitary transformation of the underlying basis [10]. Unlike the exchange of particle labels, which in fermionic systems leads to the aforementioned antisymmetric representation of $\mathcal{S}_n$ (and trivially realised using Slater determinants), such exchange of orbitals leads to transformations that span much larger irreducible representations of $\mathcal{S}_n$—in general the dimensions of these irreducible representations scale combinatorially with the number of orbitals in the problem. In this paper, we investigate the effect that different orderings of orbital or

lattice sites have on the structure of the Hamiltonian and its eigenfunctions in a spin-adapted basis. It can be expected that, for a particular system, an "optimal" permutational ordering can be found in which the exact (e.g., ground-state) wave function can be expressed most compactly—indicated by a largely increased weight of the leading coefficient in the wave function.

The effect of permutations of orbital/site indices can be seen as a similarity transformation of the Hamiltonian with an orthogonal permutation matrix $\hat{T}$, connecting the ordering schemes [11]

$$e^{-\hat{T}}\hat{H}e^{\hat{T}} = \bar{H}. \tag{1}$$

There is no change of the spectrum of $\bar{H}$, but (in contrast to a SD formulation) the explicit form of $\bar{H}$ does change in a spin-adapted basis, as we show in this paper. The influence of orbital/site ordering on the structure of the wave function was already observed in the application of the spin-adapted full configuration interaction quantum Monte Carlo (GUGA-FCIQMC) method [12,13] to lattice systems [14]. However, the interplay between orbital type, ordering, and the unitary group, and their effects on the compactness of many-body wave functions was discovered in our laboratory while solving *ab initio* Hamiltonians for ground and excited states of polynuclear transition metal clusters, exemplified by iron-sulfur clusters (dimers and cubanes) [15–17], and manganese-oxygen trinuclear molecular systems [18]. We found physically and chemically motivated (molecular) orbital transformations, based on localization and reordering, that, in the case of 1D spin systems, yield an increased compactness of the ground- and excited-state wave functions, indicated by an increased weight of the dominant basis state in the corresponding wave-function expansions. This effect is extremely beneficial for spin-adapted methods that take advantage of the sparseness of the wave function, including GUGA-FCIQMC, as the associated computational costs are dramatically reduced.

In this paper, we study the combined effect of the symmetric group $\mathcal{S}_n$ in the form of the permutations of orbital labels and the unitary group U(n) providing a spin-adapted basis, (mainly) for the spin-$\frac{1}{2}$ Heisenberg model. Such systems exhibit large quantum (spin) fluctuations compared to the above mentioned iron-sulfur clusters and manganese-oxygen *ab initio* systems, in which the effective spin on each site is quite large (e.g., $S = 5/2$), and therefore the benefit of such transformations is not immediately obvious. Nevertheless, we find that optimal orderings do exist that both compactify the exact ground-state wave function and in addition lead to a kind of mean-field solution whose physical properties, such as spin-spin correlation functions, are very close to the fully-correlated exact solutions. We will show a clear difference between the optimal orderings found for density matrix renormalization group (DMRG) and the one for compressing the many-body wave function within the UGA. We find that, unlike in DMRG, it is not locality and entanglement that determine the optimal ordering for the cumulatively spin-coupled UGA wave function, but a mechanism reminiscent of renormalization. As shown in our earlier investigations and in this paper, this finding is very general, and will be shown

here for the Hubbard model and a chemical *ab initio* model, exemplified by a chain of hydrogen atoms.

The remainder of this paper is structured as follows: In Sec. II we briefly introduce and summarize the Heisenberg model and present its spin-free form in terms of UGA operators in Sec. III. To make the elusive effect of orbital label reordering on the form of the Hamiltonian more tangible, we explicitly discuss the eigenfunctions of the 3- and 4-site Heisenberg model in the UGA formalism and the action of permutation operators on the form of the Hamiltonians and eigenfunctions in Sec. IV. We extend this concept to larger system sizes in Sec. IV A, present the results of our exhaustive search study of all possible permutations up to 10 lattice sites in Sec. IV B and investigate the spin-spin correlation functions within this framework in Sec. IV C. We show the positive results of the more compact eigenvectors due to orbital label reordering within GUGA-FCIQMC calculations for the one-dimensional Heisenberg model in Sec. V and show the results of the extension of this concept to a more general Hubbard model and an *ab initio* model system in the form of a 1D chain of hydrogen atoms in Sec. V A. Finally, we compare our reordering scheme to reorderings within the DMRG approach in Sec. V B, before we conclude in Sec. VI.

II. THE HEISENBERG MODEL

The Heisenberg model [19–23] describes the interaction of localized quantum-mechanical spins on a lattice and is a long-studied model, used to describe various aspects of magnetism in the solid state [24–35]. It is given by the Hamiltonian

$$\hat{H} = \sum_{ij}^{n} J_{ij}\hat{\mathbf{S}}_i \cdot \hat{\mathbf{S}}_j, \quad \text{with} \quad \hat{\mathbf{S}}_i = \left\{\hat{S}_i^x, \hat{S}_i^y, \hat{S}_i^z\right\}, \tag{2}$$

where the indices i and j run over all n lattice sites, $J_{ij} = J_{ji}$ are the symmetric exchange constants, and $\hat{\mathbf{S}}_i$ are the quantum mechanical spin operators with the corresponding quantum number $s \in \{\frac{1}{2}, 1, \frac{3}{2}, \dots\}$. In this paper we focus on the $s = \frac{1}{2}$ Heisenberg model with isotropic antiferromagnetic, $J_{ij} = J > 0$, nearest-neighbor (NN) interactions only, indicated by the summation subscript $\langle i, j \rangle$ in the rest of this paper.

The one-dimensional (1D) Heisenberg model with NN interaction is exactly solvable via the Bethe Ansatz [36–38], while an exact solution for higher dimensions and/or long-range interactions is still an elusive problem [39]. In 1D systems matrix product state (MPS) based methods [40–43], like the DMRG approach [44–46] are very successful, even with periodic boundary conditions (PBC) [47,48] and long-range interactions, due to the area law entanglement [49–51], while for higher dimensions tensor network state approaches can be applied [52–56]. The model does not posses a sign problem [57–59] for unfrustrated bipartite lattices [33,60] and thus quantum Monte Carlo [61–85] and more recent neural network-based approaches [86–96] are highly effective in providing very accurate numerical solutions in higher dimensions.

The total SU(2) spin symmetry of the Heisenberg model is used in the work of Flocke and Karwowski [11,97–101] using the symmetric group approach (SGA) [102–106],

in spin-symmetry adapted MPS/DMRG studies [107–115], like the interaction-round-a-face DMRG [111,116,117], density matrix based methods [118,119], and occasionally in ED [120–122] and real-space renormalization group studies [123]. Albeit the technically impractical implementations [39,121], the theoretical advantages of using a description conserving both the magnetization m_s and the total spin S are striking: (a) further reduction of the Hilbert space size (by additional block diagonalization of $\hat{H}$), (b) optimization of electronic states of desired spin, and (c) separation of nearly degenerate states of different total spin.

There are multiple ways to create a total spin-adapted basis or the so-called configuration state functions (CSFs), see Refs. [105,106] and references therein. One of them is the above mentioned SGA, which relies on the invariance of the Hamiltonian with respect to permutations of electrons, or spins in the case of the Heisenberg model [100], and its connection to the symmetric group $\mathcal{S}_n$, being the group of all permutations of n elements. A different way to construct a spin-adapted basis, which we use in this paper, is the UGA, pioneered by Paldus [4–7] and Shavitt [124–128], which relies on the spin-free formulation of the electronic structure problem [129,130]. Based on Shavitt's graphical extension to UGA (GUGA) [124–128], we recently implemented a spin-adapted version of the FCIQMC method [12–14,17,131,132], which we use in this paper to study large systems beyond the capabilities of exact diagonalization.

To some extent the influence of the ordering of orbitals in the GUGA was already noticed at its inception by Shavitt [126] and Brooks and Schaefer [133,134]. However, this was mostly to circumvent technical limitations of the time and did not concern any possible effect on the compactness of the ground-state wave function.

III. THE SPIN-FREE HEISENBERG MODEL

The Heisenberg Hamiltonian, see Eq. (2), can be expressed entirely in terms of the spin-free excitation operators $\hat{E}_{ij} = \sum_{\sigma=\uparrow,\downarrow} a^{\dagger}_{i\sigma} a_{j\sigma}$, also called shift, replacement, or singlet operators [104,135–137], as follows:

$$\hat{H} = -\frac{J}{2} \sum_{\langle ij \rangle} \hat{e}_{ij,ji} - \frac{JN_b}{4}, \qquad (3)$$

where N_b is the number of bonds in the lattice and $\hat{e}_{ij,ji} = \hat{E}_{ij}\hat{E}_{ji} - \delta_{jj}\hat{E}_{ii}$. The operator $\hat{E}_{ij}$ moves an electron or spin from lattice site j to i and fulfills the same commutation relations, $[\hat{E}_{ij}, \hat{E}_{kl}] = \delta_{kj}\hat{E}_{il} - \delta_{il}\hat{E}_{kj}$, as the generators of the unitary group [136]. $\hat{e}_{ij,ji}$ acts on the GUGA basis states given by CSFs $|\mu\rangle$ (with a specific total spin S) and can be interpreted as the UGA-version of the Heisenberg exchange operator $\hat{S}^+_i \hat{S}^-_j + \hat{S}^-_i \hat{S}^+_j$, see Appendix A for more details. Flocke and Karwowski [11] employed the related SGA to study the Heisenberg model in a spin-adapted way. The analogy between the SGA and UGA formulation of the Heisenberg Hamiltonian is reviewed in Appendix B. Equation (3) allows us to study the Heisenberg model in a spin-adapted formalism via the UGA, as utilized in the GUGA-FCIQMC method.

IV. SPIN EIGENFUNCTIONS AND THE ACTION OF PERMUTATION OPERATORS

The Hilbert space of a n-site spin-$\frac{1}{2}$ Heisenberg model can be subdivided according to the spin magnetization m_s of the system. From these states $g(n, S) = \binom{n}{n/2-S} - \binom{n}{n/2-S-1}$ spin eigenfunctions [105] with total spin S and $m_s = S$ can be constructed. The set forms a g-dimensional *irreducible* representation of the permutational group [138]. In this section we outline, through some simple examples, the consequences of this fact, which we will later exploit more generally.

Spin eigenfunctions or CSFs can be constructed *geneologically* [105,139] using the addition theorem of angular momentum. Thus an n-electron CSF with total spin S can be constructed from an $(n-1)$-electron CSF with spin $S \pm \frac{1}{2}$, by positively or negatively spin-coupling with a spin $s = \frac{1}{2}$. In this paper, we follow the common convention to label a positive spin coupled site, $\Delta S = +\frac{1}{2}$, with the symbol u and a negative, $\Delta S = -\frac{1}{2}$, with d. This must not be confused with basis states only conserving m_s, like SDs, where individual sites/spins are labeled by an up- ($\uparrow$) or down-spin ($\downarrow$) symbol. In the GUGA method, this construction is carried out cumulatively, starting with a single spin, and adding one spin at a time, until the n-electron CSF is constructed. An n-electron CSF is therefore denoted as a string of n u's and d's, such as $|uudd\rangle$. At each intermediate step, say step i, a pure-spin CSF is obtained, with cumulative spin $S_i = \sum_j^i \Delta S_j \geqslant 0$. This means that first element of the CSF string must be a u, and at each step of this cumulative construction, the number of d's cannot exceed that of u's. Also, the final cumulative spin $S_n = S$.

We now clarify our approach with the example of a 3-site Heisenberg model with open boundary conditions (OBC) with the Hamiltonian,

$$\hat{H} = \hat{\mathbf{S}}_1 \cdot \hat{\mathbf{S}}_2 + \hat{\mathbf{S}}_2 \cdot \hat{\mathbf{S}}_3, \qquad (4)$$

for $J = 1$. We call the intuitive (1-2-3) labeling of the lattices sites as the *natural* ordering. For $n = 3$ sites there are $n! = 6$ possible orderings, but for ease of demonstration we only consider the (1-3-2) ordering as an alternative for now. The natural (1-2-3) ordering is connected to the (1-3-2) ordering by the permutation operator $\hat{P}_{23}$, which exchanges labels (2) and (3), $\hat{P}_{23}(1\text{-}2\text{-}3) = (1\text{-}3\text{-}2)$.

We first look into the 3-site Heisenberg model in a m_s-adapted basis, referred to as SDs in the remainder of this paper. Without loss of generality we look at the $m_s = +\frac{1}{2}$ subspace of the 3-site Heisenberg model, which consists of three basis states, $|\uparrow\uparrow\downarrow\rangle$, $|\uparrow\downarrow\uparrow\rangle$ and $|\downarrow\uparrow\uparrow\rangle$.

The Hamiltonian $\hat{H}_{SD}$, and ground state $|\Psi^{SD}_0\rangle$ in this basis are given by,

$$\hat{H}_{SD} = -\frac{1}{2}\begin{pmatrix} 0 & 1 & 0 \\ 1 & 1 & 1 \\ 0 & 1 & 0 \end{pmatrix}, \quad |\Psi^{SD}_0\rangle = \frac{1}{\sqrt{6}}\begin{pmatrix} 1 \\ 2 \\ 1 \end{pmatrix}. \quad (5)$$

$\hat{H}_{SD}$ has one quartet ($S = \frac{3}{2}$) and two $S = \frac{1}{2}$ doublets, where the ground state with energy, $E_0 = -1.0$, is given in Eq. (5). The basis state $|\uparrow\downarrow\uparrow\rangle$ has the largest coefficient of $c_2 = \frac{2}{\sqrt{6}}$ in the ground state given in Eq. (5). The action of the permutation operator $\hat{P}_{23}$ on the SD basis states exchanges the orbital

labels (2) and (3) and is given by (we add the explicit site label)

$$\hat{P}_{23} \left| \uparrow_1 \uparrow_2 \downarrow_3 \right\rangle = \left| \uparrow_1 \uparrow_3 \downarrow_2 \right\rangle = - \left| \uparrow_1 \uparrow_2 \downarrow_3 \right\rangle, \quad (6)$$

$$\hat{P}_{23} \left| \uparrow_1 \downarrow_2 \uparrow_3 \right\rangle = \left| \uparrow_1 \downarrow_3 \uparrow_2 \right\rangle = - \left| \uparrow_1 \uparrow_2 \downarrow_3 \right\rangle, \quad (7)$$

$$\hat{P}_{23} \left| \downarrow_1 \uparrow_2 \uparrow_3 \right\rangle = \left| \downarrow_1 \uparrow_3 \uparrow_2 \right\rangle = - \left| \downarrow_1 \uparrow_2 \uparrow_3 \right\rangle, \quad (8)$$

where we added the explicit site labels as subscripts. The last equalities in Eqs. (6)–(8) come due to bringing the states back to natural ordering and the negative sign thus stems from the exchange of two fermions in this process. The matrix representation of the action of $\hat{P}_{23}$ on the SD basis states is thus given by

$$\hat{P}_{23}^{SD} = - \begin{pmatrix} 0 & 1 & 0 \\ 1 & 0 & 0 \\ 0 & 0 & 1 \end{pmatrix} = (\hat{P}_{23}^{SD})^{-1}. \quad (9)$$

We can now determine the effect of the permutation of orbital/site indices by the unitary/similarity transformation of $\hat{H}_{SD}^{123}$ (superscripts of $\hat{H}$ indicate the ordering),

$$(\hat{P}_{23}^{SD})^{-1} \cdot \hat{H}_{SD}^{123} \cdot \hat{P}_{23}^{SD} = \hat{H}_{SD}^{132}, \quad (10)$$

which explicitly reads as

$$-\frac{1}{2} \begin{pmatrix} 0 & 1 & 0 \\ 1 & 0 & 0 \\ 0 & 0 & 1 \end{pmatrix} \cdot \begin{pmatrix} 0 & 1 & 0 \\ 1 & 1 & 1 \\ 0 & 1 & 0 \end{pmatrix} \cdot \begin{pmatrix} 0 & 1 & 0 \\ 1 & 0 & 0 \\ 0 & 0 & 1 \end{pmatrix}$$
$$= -\frac{1}{2} \begin{pmatrix} 1 & 1 & 1 \\ 1 & 0 & 0 \\ 1 & 0 & 0 \end{pmatrix}, \quad (11)$$

which, except for an exchange of rows and corresponding columns, leaves the Hamiltonian representation in a SD basis, $\hat{H}_{SD}$, invariant.

We now turn to a spin-adapted basis in form of CSFs, where for an $n = 3$ system with $S = \frac{1}{2}$, there are $g = 2$ CSFs, given by $|uud\rangle$ and $|udu\rangle$. CSFs, $|\mu\rangle$, can be expressed as a linear combination of SDs, $|I\rangle$, as $|\mu\rangle = \sum_I c_I |I\rangle$, and explicit construction rules can be found, e.g., in Refs. [126,140]. Accordingly, the two $S = \frac{1}{2}$ CSFs of the 3-site Heisenberg model can be expanded as

$$|u_1 u_2 d_3\rangle = \frac{1}{\sqrt{6}} (|\uparrow_1 \downarrow_2 \uparrow_3\rangle + |\downarrow_1 \uparrow_2 \uparrow_3\rangle - 2 |\uparrow_1 \uparrow_2 \downarrow_3\rangle), \quad (12)$$

$$|u_1 d_2 u_3\rangle = \frac{1}{\sqrt{2}} (|\uparrow_1 \downarrow_2 \uparrow_3\rangle - |\downarrow_1 \uparrow_2 \uparrow_3\rangle), \quad (13)$$

where we again indicated the underlying (natural) lattice ordering as subscripts.

Because of the cumulative spin-coupling, it is not directly obvious how the permutation operator $\hat{P}_{23}$ acts on a CSF $|\mu\rangle$. To determine its action we can, however, use the expansion in terms of SDs, Eqs. (12) and (13). We show the example for $|uud\rangle$ explicitly here:

$$\hat{P}_{23} |u_1 u_2 d_3\rangle = \hat{P}_{23} \frac{1}{\sqrt{6}} (|\uparrow_1 \downarrow_2 \uparrow_3\rangle + |\uparrow_1 \downarrow_2 \uparrow_3\rangle - 2 |\downarrow_1 \uparrow_2 \uparrow_3\rangle)$$
$$= \frac{1}{\sqrt{6}} (|\uparrow_1 \downarrow_3 \uparrow_2\rangle + |\downarrow_1 \uparrow_3 \uparrow_2\rangle - 2 |\uparrow_1 \uparrow_3 \downarrow_2\rangle)$$

$$= \frac{1}{\sqrt{6}} (2 |\uparrow_1 \downarrow_2 \uparrow_3\rangle - |\uparrow_1 \uparrow_2 \downarrow_3\rangle - |\downarrow_1 \uparrow_2 \uparrow_3\rangle), \quad (14)$$

where the last line again stems to exchanging the last two spins to come back to natural ordering. Equation (14) can be expressed as

$$\hat{P}_{23} |u_1 u_2 d_3\rangle = |u_1 u_3 d_2\rangle = \frac{1}{2} |u_1 u_2 d_3\rangle + \frac{\sqrt{3}}{2} |u_1 d_2 u_3\rangle \quad (15)$$

using Eqs. (12) and (13). Similarly, the action of P_{23} on $|u_1 d_2 u_3\rangle$ yields

$$\hat{P}_{23} |u_1 d_2 u_3\rangle = |u_1 d_3 u_2\rangle = \frac{\sqrt{3}}{2} |u_1 u_2 d_3\rangle - \frac{1}{2} |u_1 d_2 u_3\rangle, \quad (16)$$

and thus the matrix representation of $\hat{P}_{23}$ acting in the Hilbert space of the $S = \frac{1}{2}$ CSFs for the 3-site Heisenberg model reads as

$$\hat{P}_{23}^{CSF} = \begin{pmatrix} \frac{1}{2} & \frac{\sqrt{3}}{2} \\ \frac{\sqrt{3}}{2} & -\frac{1}{2} \end{pmatrix} = (\hat{P}_{23}^{CSF})^{-1}. \quad (17)$$

In the natural order (1-2-3), the $S = \frac{1}{2}$ sector of the Hamiltonian is represented as

$$\hat{H}_{CSF}^{123} = - \begin{pmatrix} \frac{1}{4} & \frac{\sqrt{3}}{4} \\ \frac{\sqrt{3}}{4} & \frac{3}{4} \end{pmatrix}, \quad |\Psi_0^{CSF}\rangle = \frac{1}{2} \begin{pmatrix} 1 \\ \sqrt{3} \end{pmatrix}, \quad (18)$$

where we also indicated the CSF ground-state wave function, $|\Psi_0^{CSF}\rangle$ with energy, $E_0 = -1.0$, the second basis state, $|1\rangle = |u_1 d_2 u_3\rangle$, has the larger coefficient of $c_1 = \frac{\sqrt{3}}{2}$.

Using the matrix representation of $\hat{P}_{23}^{CSF}$, Eq. (17), we can determine the CSF Heisenberg Hamiltonian in the (1-3-2) ordering with

$$(\hat{P}_{23}^{CSF})^{-1} \cdot \hat{H}_{CSF}^{123} \cdot \hat{P}_{23}^{CSF} = \hat{H}_{CSF}^{132}, \quad (19)$$

which is given as

$$\hat{H}_{CSF}^{132} = - \begin{pmatrix} \frac{1}{2} & \frac{\sqrt{3}}{2} \\ \frac{\sqrt{3}}{2} & -\frac{1}{2} \end{pmatrix} \cdot \begin{pmatrix} \frac{1}{4} & \frac{\sqrt{3}}{4} \\ \frac{\sqrt{3}}{4} & \frac{3}{4} \end{pmatrix} \cdot \begin{pmatrix} \frac{1}{2} & \frac{\sqrt{3}}{2} \\ \frac{\sqrt{3}}{2} & -\frac{1}{2} \end{pmatrix}$$
$$= \begin{pmatrix} -1 & 0 \\ 0 & 0 \end{pmatrix}, \quad (20)$$

which means in the (1-3-2) ordering it is *already diagonal*, with the ground-state energy $E_0 = -1.0$ and ground-state wave function $|\Psi_0^{CSF}\rangle = \begin{pmatrix} 1 \\ 0 \end{pmatrix}$. Therefore, through a process of mere site re-ordering in the CSFs, we have diagonalized the Hamiltonian, meaning that a single CSF, $|u_1 u_3 d_2\rangle$, is able to fully capture the exact groundstate of the Hamiltonian in this spin sector of the Hamiltonian. By this we mean a more *compact* ground-state wavefunction, which as an extreme case consists only of one CSF in the 3-site Heisenberg model. We note that the 3-site Heisenberg chain with PBC can as well be brought to diagonal form with the same (1-3-2) ordering. As the two representations of $\hat{H}$ in Eq. (18) and Eq. (20) are related by a similarity transformation generated by the orthogonal permutation matrix connecting the ordering schemes [11], see Eq. (1), the eigenvalues do not change, while the eigenvectors undergo a very advantageous compression.

Moving to the 4-site Heisenberg chain with PBC, we find a similar behavior. Here the Hamiltonian is given by

$$\hat{H} = \hat{\mathbf{S}}_1 \cdot \hat{\mathbf{S}}_2 + \hat{\mathbf{S}}_2 \cdot \hat{\mathbf{S}}_3 + \hat{\mathbf{S}}_3 \cdot \hat{\mathbf{S}}_4 + \hat{\mathbf{S}}_4 \cdot \hat{\mathbf{S}}_1. \tag{21}$$

The $S = 0$ CSF Hilbert space is still only 2 dimensional [$g(4, 0) = 2$], with the two states $|uudd\rangle$ and $|udud\rangle$. Employing the natural order 1-2-3-4, we obtain the Hamiltonian

$$H^{1234} = -\begin{pmatrix} \frac{1}{2} & \frac{\sqrt{3}}{2} \\ \frac{\sqrt{3}}{2} & \frac{3}{2} \end{pmatrix} \tag{22}$$

whilst the order 1-3-2-4 yields the diagonal Hamiltonian

$$H^{1324} = -\begin{pmatrix} 2 & 0 \\ 0 & 0 \end{pmatrix}, \tag{23}$$

implying once again single-CSF exact eigenstates. We use the 3-site and 4-site (the latter with PBC) chain here as an illustrative example and edge case, where the corresponding Heisenberg Hamiltonians are brought into diagonal form with a "maximally compact" ground state with only one CSF. To clarify, a n-electron CSF with spin S is not *in general* a eigenfunction of the $s = 1/2$ Heisenberg Hamiltonian. Their defining characteristic is that these CSFs are eigenfunctions of the total spin operator $\hat{\mathbf{S}}^2$. CSFs are a possible basis in which the eigenfunctions of the Heisenberg Hamiltonian can be expressed (as a linear combination of CSFs) and in the special case of the 3-site (both OBC and PBC) and 4-site (with PBC) Heisenberg Hamiltonian, with proper ordering of the orbitals (the compact ordering we talk about) a single CSF is an eigenfunction/groundstate of the Heisenberg Hamiltonian. The 4-site chain with OBC and any other chain/ring with size $n > 4$ cannot be brought into purely diagonal form by a permutation of site labels. Nevertheless, as we shall show below, the underlying site ordering greatly influences the weight and nature of the CSF with the largest weight in the ground-state wave function (called the "reference" or "leading" CSF from here on). It is precisely this interplay between permutations of site indices, represented by the symmetric group $\mathcal{S}_n$, and the spin-adapted basis given by the unitary group approach, U(n), which we investigate in this paper.

We also note that Flocke and Karwowski [11] briefly mention the effect of the numbering of the lattice sites on the SGA in their 1997 paper. They found that the ordering affects the number of necessary matrix multiplications to construct a transposition (i, j). They illustrated the effect on a 4×2 square lattice (ladder), and although we focus on 1D systems in this work, we checked that Flocke and Karwowski [11] find a different ordering compared to our case. They were motivated to minimize the number of matrix multiplications to construct the transposition (i, j), see the Supplemental Material [141], whereas our motivation is to find representations in which the exact wave functions assume maximally compact forms.

A. Extension to larger systems

We now discuss how this lattice site reordering affects the ground-state wave function in a spin-adapted CSF basis for larger Heisenberg chains. To find the ordering that leads to the "most compact" ground-state description within a CSF basis, we perform ED calculations and identify the CSF with the highest weight in the ground-state wave function and compare

TABLE I. Lattice orderings for the 6-site Heisenberg model and the leading CSFs with the highest weight in the respective ground-state wave function. We also show the coefficient of the Néel state in the spin-basis for comparison.

Order		Leading CSF	Coefficient (%)	
			PBC	OBC
Natural	1-2-3-4-5-6	$|u_1 d_2 u_3 d_4 u_5 d_6\rangle$	77.9	92.2
Bipartite	1-3-5-2-4-6	$|u_1 u_3 u_5 d_2 d_4 d_6\rangle$	95.7	89.9
Compact	1-3-2-5-4-6	$|u_1 u_3 d_2 u_5 d_4 d_6\rangle$	97.1	94.7
SDs Néel state		$|\uparrow_1 \downarrow_2 \uparrow_3 \downarrow_4 \uparrow_5 \downarrow_6\rangle$	47.9	44.9

it across all possible permutations. Such a more compact wave function form, indicated by an increased weight of the dominant basis state, is very beneficial for methods like FCIQMC, see Sec. V, by facilitating the solution of a problem and extending the applicability to larger system sizes. This is also of general interest, as this procedure is not restricted to the Heisenberg model, but is very general and of broad applicability, as we have shown in Refs. [15,16] for the general nonrelativistic *ab initio* molecular Hamiltonian in the case of a nitrogen dimer and an iron-sulfur cubane chemical model system.

Because of the factorial growth of the number of possible reorderings with the system size, it is important to have a physically-motivated approach for the permutations of lattice site labels for larger lattices. A possible choice for a 6-site chain with open boundary conditions, or ring with PBC, would be a "bipartite" ordering. This ordering is motivated by the bipartite structure of the underlying lattice, which allows to subdivide the lattice into two sublattices A and B, where each site of lattice A has only neighbors belonging to lattice B and vice versa. A "bipartite ordering" arranges first all sites of lattice A followed by sites of lattice B and one possible bipartite ordering is given by, e.g., (1-3-5-2-4-6). Indeed, such a reordering, increases the weight of the most dominant CSF, given by $|u_1 u_3 u_5 d_2 d_4 d_6\rangle$ to 95.7% compared to the natural order reference state $|u_1 d_2 u_3 d_4 u_5 d_6\rangle$ with a weight of 77.9% for PBC. However, for OBC, this bipartite ordering actually decreases the weight of the leading CSF to 89.9% compared with 92.2% for the natural ordering (see Table I).

Very interestingly, we find that there exists an even "more optimal" ordering, which we term *compact* ordering, shown in Fig. 1, to be explained in the following: Let us take a closer look at the (1-3-2) and (1-3-2-4) orderings of the 3- and 4-site lattices. The (1-3-2) ordering in the 3-site OBC case leads to a single-CSF doublet ground state, and this fact is responsible for the massively increased weight of the leading CSF also in larger 1D Heisenberg systems. As we are dealing with a $S = \frac{1}{2}$ Heisenberg model, each physical site is locally a doublet. Similar to renormalization group approaches [142–145], one can interpret that the first three sites under the ordering (1-3-2) are coupled to a doublet state $S = \frac{1}{2}$ with the CSF $|uud\rangle$, termed "three-site meta-spins $\frac{1}{2}$" by Malrieu [143], and reminiscent of the block spin idea by Kadanoff [146] (see Fig. 2). To confirm this, we measured the *local spin* expectation value of the first three sites (described in the Appendix of Ref. [17]) and obtained a value that is very close to the expected value of 3/4 for a doublet $\langle(\hat{\mathbf{S}}_1 + \hat{\mathbf{S}}_3 + \hat{\mathbf{S}}_2)^2\rangle \approx 0.751$.
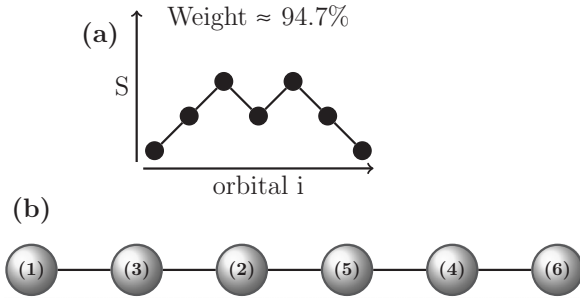
FIG. 1. Weight of leading CSF for the compact ordered 6-site chain with OBC. The labels on the lattice sites refer to the order in which the spins are coupled in the GUGA CSF formalism. Thus, for example, the second site from left with label "3" is coupled in the 3rd position in the CSF.

Thus, if we interpret sites (1-3-2) now as a renormalized site **1'**, we can again couple three "sites", (**1'**-5-4) to a new doublet with index **2'**, again with $|\mathbf{u'}ud\rangle$, where $\mathbf{u'}$ indicates the renormalized doublet. Finally, for the 6-site system the renormalized doublet couples to singlet with the remaining 6th site, yielding the total reference CSF as $|u_1u_3d_2u_5d_4d_6\rangle$. This process is schematically displayed in Fig. 2 and the corresponding site ordering and genealogical spin-coupling of the leading CSF in the compact ordering are shown in Fig. 1. The weight of this CSF in the compact ordering is 97.1% for PBC and 94.7% for OBC in the 6-site lattice, a much larger weight as compared to both the natural and bipartite orderings (see Table I).

One important difference emerges from the comparison of the natural ordering and the compact renormalized ordering. In the natural ordering the leading CSF ($|ududud\rangle$) is such that at every second site the cumulative spin vanishes ($S_i = 0$). The long-range spin correlation is therefore transferred to the other CSFs of the ground-state wave function. In the compact renormalized ordering the cumulative total spin S_i in the leading CSF is never zero at any lattice site i, $S_i > 0$ (except for the last site for a total $S = 0$ state with an even number of sites). We describe this feature as a *propagating doublet* along the chain. Thus, already the leading CSF carries information on the long-range correlation. This aspect will be discussed further in the following.
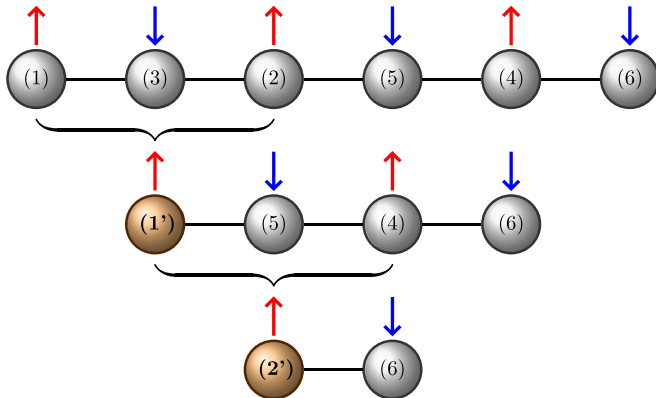

FIG. 2. Cumulative doublet coupling of "meta-spin-$\frac{1}{2}$" in the most compact order.

An expression for a total n-electron singlet CSF $|u(ud)^{\frac{n-2}{2}}d\rangle$, arising from the coupling of the propagating doublet with the last spin, reads in second quantized form:

$$\Psi_n^{S=0} = \frac{1}{\sqrt{2}}[\psi_{(n-1)\uparrow}a_{n\downarrow}^\dagger - \psi_{(n-1)\downarrow}a_{n\uparrow}^\dagger], \qquad (24)$$

where $a_{i\sigma}^\dagger$ is a creation operator at (ordered) position i with spin $\sigma \in \{\uparrow, \downarrow\}$ and $\psi_{i\sigma}$ is the propagating doublet defined by a recurrent formula

$$\psi_{i\sigma} = C_\sigma^{uud}\psi_{(i-2)\sigma}a_{(i-1)\sigma}^\dagger a_{i\bar\sigma}^\dagger$$
$$+ C_\sigma^{udu}(\psi_{(i-2)\sigma}a_{(i-1)\bar\sigma}^\dagger + \psi_{(i-2)\bar\sigma}a_{(i-1)\sigma}^\dagger)a_{i\sigma}^\dagger \quad (25)$$

with $i \in \{3, 5, ..., n-1\}$ and base $\psi_{1\sigma} = a_{1\sigma}^\dagger$. The numerical coefficients C_σ^{uud} and C_σ^{udu} are defined by the Clebsch-Gordan coefficients $\langle s_1m_1; s_2m_2 |s_{\text{tot}}m_{\text{tot}}\rangle$ arising from the angular momenta addition as

$$C_\uparrow^{uud} = \left\langle \frac{1}{2}\frac{1}{2}; \frac{1}{2}\frac{1}{2} \Big| 11 \right\rangle\left\langle 11; \frac{1}{2}\frac{\bar{1}}{2} \Big| \frac{1}{2}\frac{1}{2} \right\rangle = \sqrt{\frac{2}{3}},$$

$$C_\downarrow^{uud} = \left\langle \frac{1}{2}\frac{\bar{1}}{2}; \frac{1}{2}\frac{\bar{1}}{2} \Big| 1\bar{1} \right\rangle\left\langle 1\bar{1}; \frac{1}{2}\frac{1}{2} \Big| \frac{1}{2}\frac{\bar{1}}{2} \right\rangle = -\sqrt{\frac{2}{3}}, \qquad (26)$$

and

$$C_\uparrow^{udu} = \left\langle \frac{1}{2}\frac{1}{2}; \frac{1}{2}\frac{\bar{1}}{2} \Big| 10 \right\rangle\left\langle 10; \frac{1}{2}\frac{1}{2} \Big| \frac{1}{2}\frac{1}{2} \right\rangle = -\sqrt{\frac{1}{6}},$$

$$C_\downarrow^{udu} = \left\langle \frac{1}{2}\frac{\bar{1}}{2}; \frac{1}{2}\frac{1}{2} \Big| 10 \right\rangle\left\langle 10; \frac{1}{2}\frac{\bar{1}}{2} \Big| \frac{1}{2}\frac{\bar{1}}{2} \right\rangle = \sqrt{\frac{1}{6}}. \qquad (27)$$

One could also think about separate coupling of sites (1-3-2) and (6-5-4) to two doublet states, and a consequent coupling of the two doublet states to an overall singlet, as described in Ref. [143]. Interestingly, for the 6-site ring, both these approaches are equivalent and lead to exactly the same Hamiltonian representation. However, as our ultimate goal is to study these systems with GUGA-FCIQMC method, we focus on the cumulative approach here.

With Eqs. (24) and (25), the described ordering is easy to generalize to larger lattice sites. Moreover, it is not restricted to a bipartite lattice with an even number of sites, but is also applicable to inherently frustrated systems with an odd number of sites, as shown for the weights of the leading CSFs for a 7-site lattice with PBCs in Table II.

B. Exhaustive search study

We confirmed our renormalization-group motivated [143,144] Ansatz, described above, by considering all $n!$ possible permutations of site labels. For all these permutations we exactly diagonalized the corresponding Heisenberg Hamiltonian and investigated what the highest weighted CSF in the ground state is. Because of the rather small Hilbert space size, we were able to exhaustively search the full n-factorial permutational space up to 10-site systems and confirm that this compact ordering holds for these system sizes. The optimal ordering for a 10-site system is (1-3-2-5-4-7-6-9-8-10) and the dominant CSF is $|u_1u_3d_2u_5d_4u_7d_6u_9d_8d_{10}\rangle$ with a 90.3% weight, which again reflects the coupling of three consecutive sites to a doublet in an iterative way, as depicted in Fig. 2.

TABLE II. 7-site orderings and leading CSF weights.

| | Order | Ref. CSF | CI coefficient (%) | |
			PBC	OBC
Natural	1-2-3-4-5-6-7	$\lvert u_1 d_2 u_3 d_4 u_5 d_6 u_7 \rangle$	79.5	67.0
Compact	1-3-2-5-4-7-6	$\lvert u_1 u_3 d_2 u_5 d_4 u_7 d_6 \rangle$	88.7	94.3
	SDs "Néel state"	$\lvert \uparrow_1 \downarrow_2 \uparrow_3 \downarrow_4 \uparrow_5 \uparrow_6 \downarrow_7 \rangle$	40.5	54.4

For systems larger than 10 sites the combinatorial growth of permutations (10! = 3628800 already) prevents an exhaustive search. At the same time obtaining the highest weighted CSF requires a diagonalization of the Hamiltonian, which also is not a feasible route to scale to bigger problems. For this reason we investigated possible cheaper indicators of an optimal ordering and the corresponding leading CSF for system sizes up to 10 sites. Figure 3 shows how the lowest diagonal matrix element (also called as single CSF energies) of the Hamiltonian corresponding to different noncyclic permutations or orderings, and the CSF with the highest weight in the wave function are connected. It is evident that the CSF corresponding to the most negative diagonal matrix element [see Fig. 3(a)] has the highest weight in the wave function [see Fig. 3(b)]. The first 4 data points correspond to 4 equivalent compact orderings, followed by 12 equivalent bipartite orderings of the site labels. The figure also shows the single CSF energies of the natural ordering and the diagonal element of a Néel state in a SD basis. One can see that there is a stark decrease of the diagonal matrix elements in the compact

FIG. 3. (a) Lowest single CSF energies and (b) corresponding weight $\lvert c_0 \rvert$ for the 6-site ring as a function of permutations. The permutations/orderings are ordered by decreasing maximum weight $\lvert c_0 \rvert$ in the ground-state wave function (only the first 100 highest weighted permutations are shown for clarity).

ordering, which is already quite close to the ground-state energy of this system. Thus, for the spin-$\frac{1}{2}$ Heisenberg model with nearest-neighbor interaction the diagonal matrix elements are an indicator for the optimal ordering, leading to the most *compact* ground-state eigenvector indicated by a substantial increased weight of the leading CSF compared to the natural ordering. Consequently, a cheaper option to find the most compact representation, other than diagonalization of the full Hamiltonian, is to minimize the diagonal matrix element over the space of possible permutations, $\mathcal{S}_n$, and CSFs, $\{\lvert \mu \rangle\}$,

$$\min_{\mathcal{S}_n} \min_{\mu} \langle \mu \lvert H \rvert \mu \rangle. \qquad (28)$$

In the GUGA-Heisenberg model the single CSF energies are given by the diagonal exchange contributions:

$$\langle \mu \lvert \hat{H} \rvert \mu \rangle \sim \frac{1}{2} \sum_{j>i} J_{ij} X_{ij}(\mu), \quad J_{ij} = \begin{cases} J & \text{for NN,} \\ 0 & \text{else,} \end{cases} \qquad (29)$$

where $X_{ij}(\mu)$ is a CSF dependent quantity and J_{ij} is nonzero for NN sites i and j depending on the chosen ordering. The explicit derivation of Eq. (29) is beyond the scope of the present manuscript and we refer the interested reader to Refs. [12,125] and specifically to Appendix A.2.1 of Ref. [14]. For NN interaction only, the task to minimize Eq. (29) for a given CSF $\lvert \mu \rangle$ is equivalent to the traveling salesman problem (TSP) [147] [after scaling the possibly negative $X_{ij}(\mu)$ to positive quantities]. This can best be seen when formulating the TSP as an integer linear program [148,149] in the Miller-Tucker-Zemlin [150] or Dantzig-Fulkerson-Johnson formulation [151]. For more general Heisenberg (higher dimension, longer and anisotropic interactions), or even *ab initio* models, the minimization of the corresponding Eq. (29) can be mapped to more general quadratic assignment problem [152].

Both quantities $X_{ij}(\mu)$ and J_{ij} can be expressed in matrix form, where the task is to construct an ordering of the 1D system, which changes J_{ij} to give the lowest possible diagonal matrix element, according to Eq. (29). Figure 4 shows $X_{ij}(\mu)$ for (a) $\lvert ududud \rangle$ with the original/natural ordering (1-2-3-4-5-6), (b) $\lvert uuuddd \rangle$ with the bipartite ordering (1-4-2-5-3-6) and (c) $\lvert uududd \rangle$ with the *compact* ordering (1-3-2-5-4-6). The optimal J_{ij} and thus orderings, which minimize the diagonal matrix element, Eq. (29), are indicated by the black rectangles/frames in Fig. 4, which act as a "mask" and determine, which X_{ij} elements contribute to the sum in Eq. (29). The direct relation between the lowest diagonal matrix element corresponding to the highest weight in the ground-state wave function can be used to implement efficient approximate solvers to find the optimal permutation and confirm our assumed renormalization structure. We implemented a simulated annealing [153–157] minimizer with
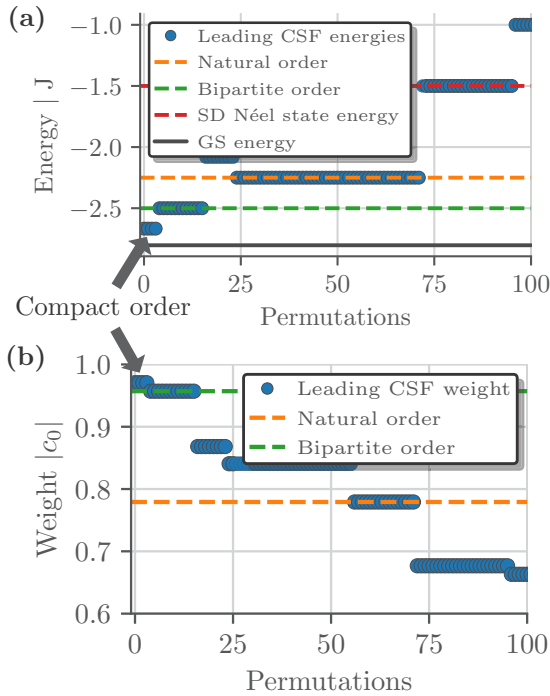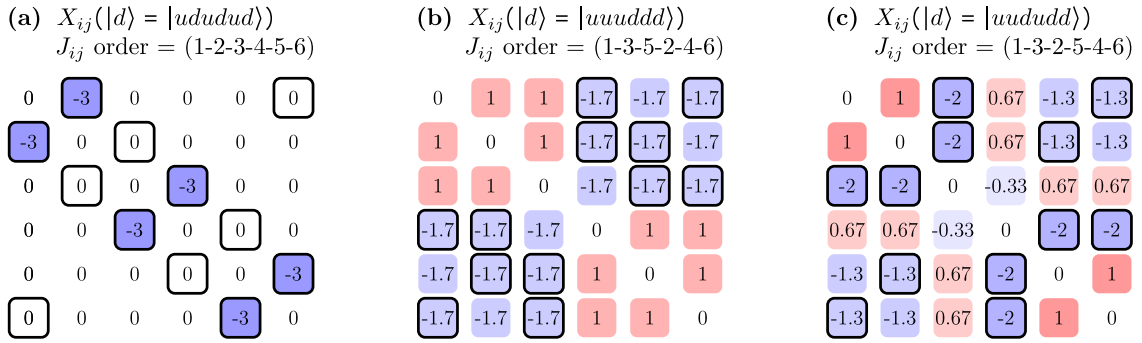
(a) $X_{ij}(|d\rangle = |ududud\rangle)$
J_{ij} order = (1-2-3-4-5-6)

0	-3	0	0	0	0
-3	0	0	0	0	0
0	0	0	-3	0	0
0	0	-3	0	0	0
0	0	0	0	0	-3
0	0	0	0	-3	0

(b) $X_{ij}(|d\rangle = |uuuddd\rangle)$
J_{ij} order = (1-3-5-2-4-6)

0	1	1	-1.7	-1.7	-1.7
1	0	1	-1.7	-1.7	-1.7
1	1	0	-1.7	-1.7	-1.7
-1.7	-1.7	-1.7	0	1	1
-1.7	-1.7	-1.7	1	0	1
-1.7	-1.7	-1.7	1	1	0

(c) $X_{ij}(|d\rangle = |uududd\rangle)$
J_{ij} order = (1-3-2-5-4-6)

0	1	-2	0.67	-1.3	-1.3
1	0	-2	0.67	-1.3	-1.3
-2	-2	0	-0.33	0.67	0.67
0.67	0.67	-0.33	0	-2	-2
-1.3	-1.3	0.67	-2	0	1
-1.3	-1.3	0.67	-2	1	0

FIG. 4. Exchange matrix elements X_{ij} for the 6-site chain reference CSFs: (a) $|ududud\rangle$ (natural), (b) $|uuuddd\rangle$ (bipartite), and (c) $|uududd\rangle$ (compact), with the respective order in parenthesis. The nonzero J_{ij} values, due to the corresponding orderings, are indicated by the black rectangles/frames. They act as a "mask" in the product $X_{ij}J_{ij}$, see Eq. (29), and for a given CSF, the "optimal" lattice ordering yields the lowest possible diagonal matrix element, Eq. (29). (Color online: blue/red colors are a guide to the eye indicating the sign and magnitude of the respective values.)

2- [158,159] and 3-opt modifications [160] based on the Lin-Kernigham heuristic [161] to find the optimal ordering for a given CSF. Additionally, the mapping to the TSP allowed us to find the optimal ordering with a state-of-the-art solver by Helsgaun [162,163] (see the Supplemental Material for sample input files [141]).

To deal with the exponentially growing Hilbert space with increasing system size we combined our excitation generation routines of FCIQMC to stochastically suggest new states, $|\nu\rangle$ for a given CSF, $|\mu\rangle$. With this approach we were able to confirm our renormalized ordering Ansatz for system sizes up to $n = 20$ (where we were still able to enumerate the whole Hilbert space), which gives us great confidence that this is not a result restricted to small system sizes. More details on our simulated annealing approach can be found in Appendix C.

C. Spin-spin correlation functions

In addition to the renormalization behavior, another physical motivation can be drawn for the dominant CSF in the optimal ordering: it shows a spin-spin correlation function similar to the exact ground-state wave function. This is possible, since a CSF, $|\mu\rangle$, consists of a linear combination of SDs [126,140,164,165], $\{|I\rangle\}$, (see Supplemental Material [141] for examples)

$$|\mu\rangle = \sum_I c_I |I\rangle, \tag{30}$$

and thus can yield nontrivial spin-spin correlation functions, even for a single CSF. Figure 5 shows three spin-spin correlation functions $\langle \hat{S}_j^z \cdot \hat{S}_x^z \rangle$, with $j = 1, 5$, and $j = 10$ and x ranging from 1 to 10 for a 10-site Heisenberg chain with OBC, for the different lattice orderings considered in this paper compared with the exact result. Both the natural and bipartite single CSF spin-correlation function show a rather trivial behavior. The former characterized by a quickly vanishing spin-spin correlation function already after the first NN, and the latter exhibiting an alternating uniform correlation function. In the case of the natural order leading CSF, $|u_1 d_2 u_3 d_4 u_5 d_6 u_7 d_8 u_9 d_{10}\rangle$, this behavior stems from the above mentioned vanishing intermediate spin, $S_i = 0$, at every other lattice site. On the contrary, already the leading CSF in the *compact* ordering carries information of the long-range spin-correlation and exhibits a spin-correlation function that resembles the exact $\langle \hat{S}_j^z \cdot \hat{S}_x^z \rangle$.

We extended this study to larger lattices, as shown in Fig. 6(a), where we find that for odd- and even lattice spacings the spin-correlation function of the compact reference CSF is exactly described by an exponential fit $\langle \hat{S}_1^z \cdot \hat{S}_x^z \rangle = a \cdot e^{-bx}$ for x even/odd [green and red dashed lines in Fig. 6(a)]. The values of the fit are given by $a_{\text{even}} = 0.153$ and $b_{\text{even}} = 0.203$ for even (excluding the first $\langle \hat{S}_1^z \cdot \hat{S}_1^z \rangle$ data point) and $a_{\text{odd}} = -1/4$ and $b_{\text{odd}} = 0.203$ for odd lattice spacings. The exact and compact-reference-CSF spin-spin correlation functions for a 30-site lattice with OBC are shown in Fig. 6(b), which shows that the single CSF results mimic the exact result even for large lattice sizes. However, the short-range behavior of the
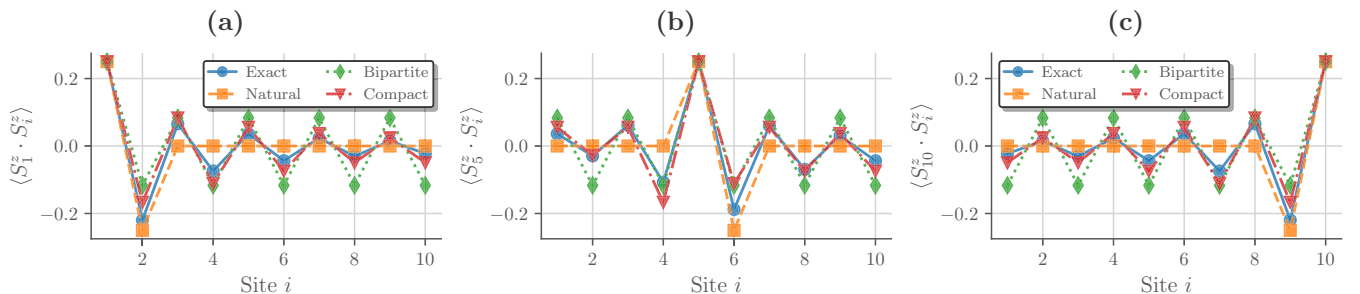

FIG. 5. (a) $\langle S_1^z \cdot S_x^z \rangle$, (b) $\langle S_5^z \cdot S_x^z \rangle$, and (c) $\langle S_{10}^z \cdot S_x^z \rangle$ exact and single-CSF spin-spin correlation functions for the 10-site chain with OBC.
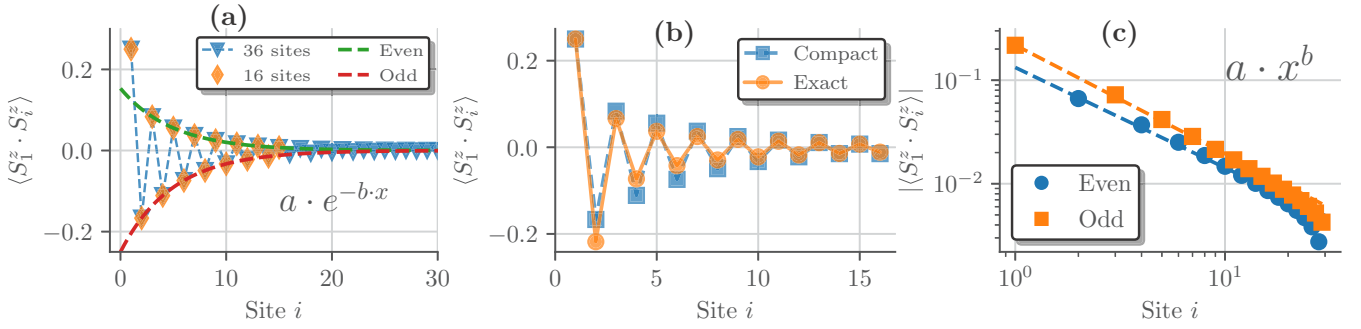
FIG. 6. (a) Single CSF spin-spin correlation function for the compact ordering vs chain size and an exponential fit to the even (green-dashed line) and odd spin-spin correlation (red-dashed line) for the 36-site single CSF in the compact order, with $a_{\mathrm{even}} = 0.153$, $b_{\mathrm{even}} = 0.203$, $a_{\mathrm{odd}} = -0.25$, and $b_{\mathrm{odd}} = 0.203$. (b) OBC Single CSF spin-spin correlation function for the compact ordering compared with exact results obtained with the $\mathcal{H}\Phi$ software package [166] for 30 sites. (c) Power fit to the even and odd spin-spin correlation for the 30-site exact spin-spin correlation function displayed on a double logarithmic scale, with $a_{\mathrm{even}} = 0.133$, $b_{\mathrm{even}} = -0.969$, $a_{\mathrm{odd}} = -0.218$, and $b_{\mathrm{odd}} = -1.049$.

exact spin-spin correlation function follows a power-law decay [39], $\langle \hat{S}_1^z \cdot \hat{S}_x^z \rangle \sim a \cdot x^b$, with $a_e = 0.133$ and $b_e = -0.969$ for even and $a_o = -0.218$ and $b_o = -1.049$ for odd lattice spacings in the 30-site case, see Fig. 6(c).

Using the method of *generating functions*, Sato *et al.* [167] found the exact thermodynamic limit results for $\langle S_1^z \cdot S_r^z \rangle$ up to $r = 7$, which are shown in Table III along the single CSF and exact diagonalization (ED) results of 30 sites with OBC. Based on the entanglement perturbation theory (EPT) approach, Wang and Chung [168], derived a relation of $A(r) = -0.1473 r^{-0.9604}$ with an error of 0.1% for the odd separations, which also fits the even sites with an opposite sign. Based on a bosonization approach, Hikihara and Furusaki [169] find a critical exponent $b = -1$. We fitted a power-law behavior to the available TDL data [167], see Fig. 7, and gathered the resulting parameters a and b in Table IV, along with the data obtained based on the compact single CSF and 30-site ED results with OBC. Even though the spin-spin correlation function based on the leading CSF of the compact ordering is exponentially decaying, as shown in Fig. 6(a), the short-range behavior, $\langle \hat{S}_j^z \cdot \hat{S}_{j+1}^z \rangle$—especially for even lattice spacings—is quite close to the exact TDL data, as shown in Fig. 7.

For this reason we also fitted the spin-spin correlation function obtained from the compact-order leading CSF with

a power law, $a \cdot x^b$, and gathered the results in Table IV. The numbers of sites in Table IV indicate how many data points of $\langle \hat{S}_i^z \cdot \hat{S}_{i+j}^z \rangle$ were taken into account for the fitting. Using only the first 18 lattices yields a critical exponent $b_{\mathrm{even}} = -0.979$ very close to the EPT result by Wang and Chung. Increasing the considered number of sites to 96, the critical exponent for even lattice separations overestimates the corresponding reference results, but b_{odd} comes closer. The fact that the spin-spin correlation function obtained by a single CSF is so close to exact many-body results is striking.

V. GUGA-FCIQMC CALCULATIONS

In this section we study the scaling of the (increased) weight of the leading CSF for lattice sizes beyond the capabilities of ED approaches (≈ 50 sites [170,171]) and the effect it has on GUGA-FCIQMC calculations, as the method usually benefits from a "more single reference and sparse" character of the sampled wave function. Details on the GUGA-FCIQMC method can be found in Appendix D and Refs. [12,13] and computational details and sample input files can be found in the Supplemental Material [141].
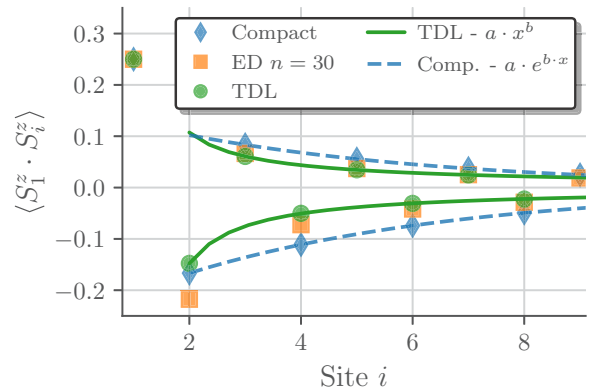
TABLE III. Spin-spin correlation function $\langle S_j^z S_{j+k}^z \rangle$ for the 30-site chain with OBC computed with the single CSF with largest weight corresponding to the compact ordering and with the full wave function obtained from an ED calculation. For comparison we also show the exact thermodynamic limit (TDL) values [167]. k indicates the neighbor.

k	Compact CSF	Exact OBC $n = 30$	Exact TDL [167]
1	-0.166667	-0.2174740	-0.1477157
2	0.083333	0.0664877	0.0606798
3	-0.111111	-0.0722632	-0.0502486
4	0.055556	0.0370753	0.0346528
5	-0.074074	-0.0417185	-0.0308904
6	0.037037	0.0251398	0.0244467
7	-0.049383	-0.0286345	-0.0224982

FIG. 7. Analytic TDL spin-spin correlation function [167] with power-law fits (solid lines) for even and odd lattice sites, with $a_{\mathrm{even}} = 0.107$, $b_{\mathrm{even}} = -0.820$, $a_{\mathrm{odd}} = -0.148$, and $b_{\mathrm{odd}} = -0.975$, compact single CSF spin-spin correlation function with exponential fit (dashed lines) and $n = 30$ exact results (ED) with OBC [166].

TABLE IV. Fit of $\langle S_0^z \cdot S_r^z \rangle$ to $a \cdot x^b$ for odd and even lattice sites.

Method	Compact CSF		ED OBC	EPT [168]	TDL [167]
# sites	18	96	30	∞	7
a_{even}	0.174	0.201	0.133		0.107
b_{even}	−0.979	−1.147	−0.969	−0.9604	−0.820
Err [%]	0.3	0.3	0.1	0.1	0.0
a_{odd}	−0.178	−0.183	−0.218	−0.1473	−0.148
b_{odd}	−0.726	−0.880	−1.049	−0.9604	−0.975
Err [%]	0.8	0.7	0.1	0.1	0.0

As we have identified the single CSF energy as a good indicator for a more optimal ordering, we show it for the different orderings in Fig. 8(a) compared to the numerically exact energy of the Heisenberg model with OBC, obtained with the $\mathcal{H}\Phi$ software package [166] (here for lattices sizes up to 30 sites) and exact Bethe Ansatz results [172] (for lattice sizes up to 64 sites) as a function of the number of sites.

It can be seen that the single CSF energy in the compact ordering is closest and in fact almost parallel to the exact energy, and thus, the leading CSF in the compact ordering yields a better "starting point" for subsequent high accuracy calculations. We demonstrate this by showing GUGA-FCIQMC results
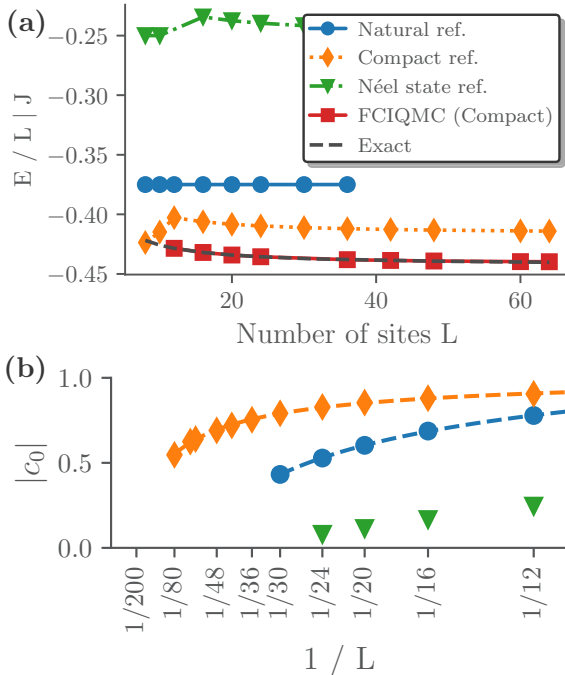

FIG. 8. (a) OBC Néel state and single CSF energies (diagonal Hamiltonian matrix element) of the natural and compact orderings vs the number of sites compared with GUGA-FCIQMC results—using a CSF basis and the compact ordering—and exact Bethe Ansatz [172] and ED results, obtained with $\mathcal{H}\Phi$ [166]. (Energies/diagonal matrix elements are divided by the corresponding number of sites L for comparative reasons.) (b) OBC weights of the Néel state and the leading CSFs of the natural and compact orderings vs the inverse lattice size obtained with GUGA-FCIQMC. These weights are an approximation of the exact $|c_0^{ex}|$ of the ground-state wave function obtained via, e.g., ED.
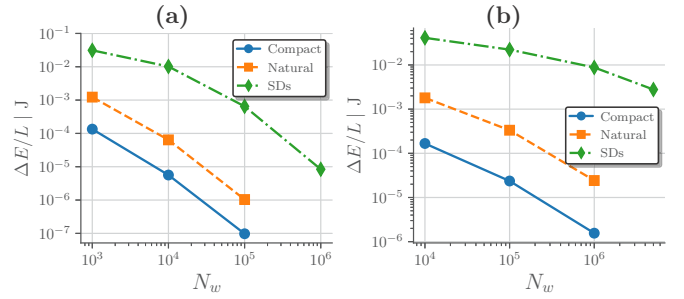

FIG. 9. Difference of GUGA-FCIQMC energy per site results compared to ED results [166] of the 20- (a) and 30-site (b) 1D Heisenberg model with OBC for different orderings (natural and compact) and a SD-based results (SDs) vs the number of walkers N_w.

obtained using the compact ordering in Fig. 8(a), which—on this scale—are not distinguishable from the analytic results. Concerning cost and accuracy, using the compact lattice ordering has a very beneficial impact on these GUGA-FCIQMC calculations as we show in Fig. 9 and discuss in more detail below.

In Fig. 8(b) we show the weights of the leading CSF, $|c_0|$, obtained from GUGA-FCIQMC calculations for the different orderings as a function of the inverse lattice size $1/L$ with OBC. The weights obtained with GUGA-FCIQMC are an approximation of the exact $|c_0^{ex}|$ of the ground-state wave function obtained via, e.g., ED. The effect that the weight of the leading CSF in the *compact* ordering is substantially larger compared to the other orderings becomes even more pronounced for larger lattices. This increased weight has a very beneficial influence on the convergence of GUGA-FCIQMC calculation for finite lattices. To demonstrate this, Fig. 9 shows the energy difference to numerically exact DMRG results, obtained with BLOCK[107,173–175], for the (a) 20- and (b) 30-site Heisenberg model with OBC for the compact and natural ordering and a SD-based calculations as a function of the number of walkers N_w.

Using the spin-adapted GUGA-FCIQMC calculation with the natural ordering is an order of magnitude more accurate for a given number of walkers N_w compared to the standard SD-based implementation. In addition, using the compact ordering yields an additional order of magnitude in accuracy. As we show below, the increased weight of the leading CSF induced by site reordering in the GUGA-scheme is not restricted to the Heisenberg model.

A. Extension to Hubbard and *ab initio* models

Here we extend our study from a pure spin-model to Fermionic problems in form of the Hubbard model and to *ab initio* Hamiltonians in form of chains of equally spaced hydrogen atoms. This entails a much larger Hilbert space size, as the orbitals/sites can also be empty or doubly occupied. The spin-free form of the Hubbard model with NN interaction in a real-space representation is given by [176]

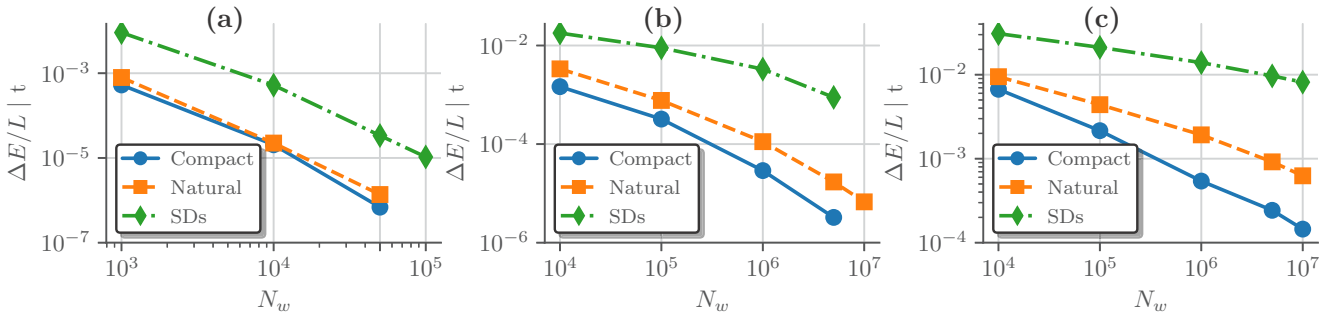$$\hat{H} = -t \sum_{\langle ij \rangle} \hat{E}_{ij} + \frac{U}{2} \sum_i \hat{e}_{ii,ii}, \quad (31)$$

FIG. 10. Difference of GUGA-FCIQMC energy per site results compared to $M = 500$ DMRG reference results [107,173–175] of the 10-(a), 20- (b), and 30-site (c) 1D Hubbard model with OBC for different orderings (natural and compact) and SD-based results (SDs) vs the number of walkers N_w.

where $\hat{E}_{ij}$ moves an electron from site j to i with hopping strength t (usually chosen as the unit of energy) and $\sum_i \hat{e}_{ii,ii}$ counts the number of doubly occupied scaled with the on-site Coulomb repulsion strength U. The general spin-free *ab initio* electronic structure Hamiltonian in the Born-Oppenheimer approximation is given by [129]

$$\hat{H} = \sum_{ij} t_{ij} \hat{E}_{ij} + \frac{1}{2} \sum_{ijkl} V_{ijkl} \hat{e}_{ij,kl}, \qquad (32)$$

with $\hat{e}_{ij,kl} = \hat{E}_{ij}\hat{E}_{kl} - \delta_{jk}\hat{E}_{il}$ and t_{ij} and V_{ijkl} are the molecular one- and two-body integrals. To stay as close as possible to our Heisenberg study above, we choose the parameters of the models in such a way (localized bases, large U/t and hydrogen atom separation) so that the ground states are dominated by states with entirely singly-occupied/open-shell orbitals.

Figures 10(a)–10(c) show the difference of GUGA-FCIQMC energy per site results compared to numerically exact DMRG results [107,173–175] for the 10-, 20-, and 30-site Hubbard model with $U/t = 16$ and OBC. Similar to the Heisenberg results, using a spin-adapted formulation and the compact ordering yields an order of magnitude more accurate results compared to a SD based calculation. Albeit not as drastic as for the Heisenberg model, also the weight of the leading CSF, $|c_0|$, is substantially increased for the Hubbard model calculations, as shown in Table V.

As an example of an *ab initio* model system, we study 1D hydrogen chains, recently studied to benchmark various computational physics and chemistry approaches [177,178]. Figures 11(a)–11(c) show the difference of GUGA-FCIQMC energy per site results compared to numerically exact DMRG calculations [107,173–175] for a 10-, 20-, and 30-site hydrogen chain in a STO-3g basis set for the different orderings and SD-based calculations as a function of the number of walkers.

The inter-hydrogen separation was 3.6 Å and we used localized orbitals. The results are very similar to the Heisenberg and Hubbard model discussed above, where again, performing spin-adapted calculations with a compact ordering yields results an order of magnitude more accurate for a given number of walkers compared to the standard SD-based FCIQMC method. In addition the compact ordering increases the weight of the leading CSF compared to the natural ordering, as shown in Table V. We would like to note that both the 30-site Hubbard and hydrogen chain are far beyond the capabilities of state-of-the-art ED approaches.

B. Comparison with DMRG reordering

It is well known that orbital reordering is crucial in DMRG. However, as discussed in our earlier studies [15,16] the reordering we seek in the context of spin couplings differs from the one in DMRG, both in motivation and in aim. In the context of DMRG, site reordering is very important for convergence with respect to the bond dimension (M), and relies on concepts of entanglement and quantum (mutual) information [173–175,179–185]. Our reordering schemes are strictly motivated by the intrinsic mechanisms of the cumulative spin couplings and aim at the compression of wave functions expanded in CSFs. The former is bound to the concept of locality, while our reordering is nonlocal.

In this section we provide a numerical proof that the best reordering in GUGA is not necessarily the best in DMRG, by analyzing the DMRG convergence using the natural and the optimal ordering for a chain of 30 hydrogen atoms. We used the BLOCK DMRG code [107,173–175], which is able to use SU(2) symmetry and allows user-defined orbital orderings. We used the standard Fiedler algorithm [183,186–188] to find the optimal order for the DMRG calculation, which yielded the natural order as a result. (Computational details and sample input files can be found in the Supplemental Material [141]) We then compared results obtained with the natural/Fiedler ordering and our "optimal" compact ordering with and without SU(2) conservation. As a reference we used a well-converged $M = 400$ result using SU(2) and natural ordering. Figure 12 shows the results of this study.

A one-dimensional hydrogen chain, with a large atom separation of 3.6 Å, is an optimal case for a MPS-based algorithm like DMRG. This is reflected in the incredibly fast convergence of the natural ordered SU(2) results with a

TABLE V. Weight of the leading CSF [%] for the Heisenberg, Hubbard and Hydrogen chains with OBC for the natural and compact ordering.

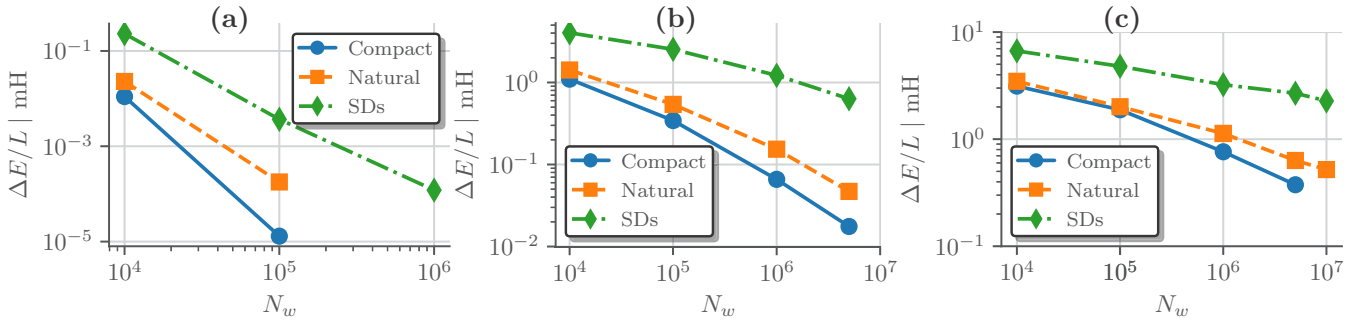| Order	Heisenberg		Hubbard			Hydrogen		
# sites	20	30	10	20	30	10	20	30
Compact	85.4	79.0	87.3	77.1	68.4	74.0	54.9	46.8
Natural	60.2	43.0	78.9	54.7	43.3	67.2	41.3	36.1

FIG. 11. Energy difference per site to the $M = 500$ DMRG reference results of the 10- (a), 20- (b), and 30-site (c) hydrogen chain in a minimal basis for different orderings (natural and compact) and SD-based results (SDs) vs the number of walkers N_w.

matrix dimension of $M = 100$. Similar to the GUGA-FCIQMC results, making use of the inherent SU(2) symmetry is very beneficial for the DMRG convergence. However, the 30-site hydrogen results indeed show a difference between the natural and the compact ordering scheme. While the natural order results with SU(2) symmetry (blue circles) are already converged for $M = 100$, the compact ordering scheme, which introduces some long-range interactions, requires a matrix dimension of $M = 400$ to converge to similar levels of accuracy ($< 10^{-2}$ mH).

This demonstrates that the optimal ordering scheme for the GUGA framework differs from the DMRG one. While the latter is based on locality and entanglement arguments, the cumulative spin-coupling in the GUGA enables the inclusion of renormalization-group concepts to render the description of strongly-correlated many-body systems more compact (a nonlocal concept).

VI. CONCLUSIONS

In this paper we demonstrate a novel combined symmetric and unitary group approach, applied to the one-dimensional spin-$\frac{1}{2}$ Heisenberg model, which yields a more compact ground-state wave function. We find that a specific ordering of the underlying lattice sites, governed by the symmetric group $\mathcal{S}_n$ combined with the cumulative spin-coupling of the
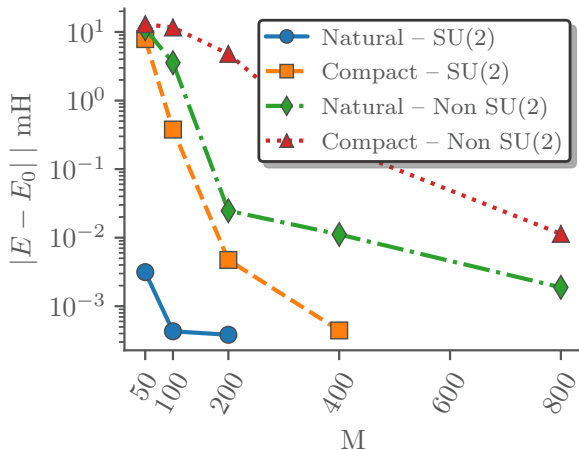

FIG. 12. 30-site hydrogen chain DMRG energy difference to $M = 500$ Fiedler (natural order) reference result for different orbital ordering with and without spin-adaptation vs matrix dimension M.

unitary group approach U(n) resembles a block-spin/real-space renormalization group. This induces a more *compact* description of the ground state where the most important CSF has a much higher weight than in the natural order. We derive an analytic formula for this compact CSF for the 1D Heisenberg model, and find a general description of this *compact* ordering, which is easily applicable to 1D lattices of arbitrary size. We find that this state, up to leading order, already captures with high accuracy the spin-spin correlation behavior of the exact ground-state wave function. A more compact ground state facilitates spin-adapted GUGA-FCIQMC calculations for larger lattice sites. We compare this compact ordering to the optimal ordering for DMRG calculations based on quantum mutual information, and find that they differ. Finally, we show that this concept also applies for more general lattice models, like the Hubbard model, and even to *ab initio* quantum chemical systems, in form of one-dimensional hydrogen chains. In future work we will investigate the utility of this combined total spin-adapted unitary and symmetric group approach in more complex systems of higher dimension and/or with long-range interaction, including frustrated spin systems.

ACKNOWLEDGMENT

APPENDIX A: THE SPIN-FREE FORMULATION OF THE HEISENBERG MODEL

Expressing the local spin operators as [6]

$$\hat{S}_i^k = \frac{1}{2} \sum_{\mu,\nu=\uparrow,\downarrow} \sigma_{\mu,\nu}^k a_{i,\mu}^\dagger a_{i\nu}, \tag{A1}$$

with the Pauli matrices [189]

$$\sigma^x = \begin{pmatrix} 0 & 1 \\ 1 & 0 \end{pmatrix}, \quad \sigma^y = \begin{pmatrix} 0 & -i \\ i & 0 \end{pmatrix}, \quad \sigma^z = \begin{pmatrix} 1 & 0 \\ 0 & -1 \end{pmatrix} \tag{A2}$$

and the fermionic annihilation (creation) operators $a_{i,\mu}^{(\dagger)}$ of electrons with spin μ in spatial orbital i. This results in the explicit expressions

$$\hat{S}_i^x = \frac{1}{2}(a_{i\uparrow}^\dagger a_{i\downarrow} + a_{i\downarrow}^\dagger a_{i\uparrow}), \tag{A3}$$

$$\hat{S}_i^y = \frac{i}{2}(a_{i\downarrow}^\dagger a_{i\uparrow} - a_{i\uparrow}^\dagger a_{i\downarrow}), \tag{A4}$$

$$\hat{S}_i^z = \frac{1}{2}(n_{i\uparrow} - n_{i\downarrow}), \tag{A5}$$

where $n_{i\mu} = a_{i\mu}^\dagger a_{i\mu}$ is the fermionic number operator of orbital i and spin μ. If we express $\hat{\mathbf{S}}_i \cdot \hat{\mathbf{S}}_j$ as

$$\hat{\mathbf{S}}_i \cdot \hat{\mathbf{S}}_j = \hat{S}_i^z \cdot \hat{S}_j^z + \hat{S}_i^x \cdot \hat{S}_j^x + \hat{S}_i^y \cdot \hat{S}_j^y \tag{A6}$$

and consequently the individual terms as

$$\hat{S}_i^z \cdot \hat{S}_j^z = \frac{1}{4}(n_{i\uparrow} - n_{i\downarrow})(n_{j\uparrow} - n_{j\downarrow}), \tag{A7}$$

$$\begin{aligned}\hat{S}_i^x \cdot \hat{S}_j^x &= \frac{1}{4}(a_{i\uparrow}^\dagger a_{i\downarrow} + a_{i\downarrow}^\dagger a_{i\uparrow})(a_{j\uparrow}^\dagger a_{j\downarrow} + a_{j\downarrow}^\dagger a_{j\uparrow})\\ &= \frac{1}{4}(a_{i\uparrow}^\dagger a_{i\downarrow} a_{j\uparrow}^\dagger a_{j\downarrow} + a_{i\uparrow}^\dagger a_{i\downarrow} a_{j\downarrow}^\dagger a_{j\uparrow}\\ &\quad + a_{i\downarrow}^\dagger a_{i\uparrow} a_{j\uparrow}^\dagger a_{j\downarrow} + a_{i\downarrow}^\dagger a_{i\uparrow} a_{j\downarrow}^\dagger a_{j\uparrow}), \end{aligned} \tag{A8}$$

$$\begin{aligned}\hat{S}_i^y \cdot \hat{S}_j^y &= -\frac{1}{4}(a_{i\downarrow}^\dagger a_{i\uparrow} - a_{i\uparrow}^\dagger a_{i\downarrow})(a_{j\downarrow}^\dagger a_{j\uparrow} - a_{j\uparrow}^\dagger a_{j\downarrow})\\ &= \frac{1}{4}(-a_{i\downarrow}^\dagger a_{i\uparrow} a_{j\downarrow}^\dagger a_{j\uparrow} + a_{i\downarrow}^\dagger a_{i\uparrow} a_{j\uparrow}^\dagger a_{j\downarrow}\\ &\quad + a_{i\uparrow}^\dagger a_{i\downarrow} a_{j\downarrow}^\dagger a_{j\uparrow} - a_{i\uparrow}^\dagger a_{i\downarrow} a_{j\uparrow}^\dagger a_{j\downarrow}), \end{aligned} \tag{A9}$$

we can combine the x and y terms as

$$\begin{aligned}\hat{S}_i^x \cdot \hat{S}_j^x + \hat{S}_i^y \cdot \hat{S}_j^y &= \frac{1}{2}(a_{i\uparrow}^\dagger a_{i\downarrow} a_{j\downarrow}^\dagger a_{j\uparrow} + a_{i\downarrow}^\dagger a_{i\uparrow} a_{j\uparrow}^\dagger a_{j\downarrow})\\ &= \frac{1}{2}\sum_\sigma a_{i\sigma}^\dagger a_{i\bar\sigma} a_{j\bar\sigma}^\dagger a_{j\sigma}. \end{aligned} \tag{A10}$$

For $i \neq j$ we can transform Eq. (A10) to

$$\hat{S}_i^x \cdot \hat{S}_j^x + \hat{S}_i^y \cdot \hat{S}_j^y = -\frac{1}{2}\sum_\sigma a_{i\sigma}^\dagger a_{j\sigma} a_{j\bar\sigma}^\dagger a_{i\bar\sigma} = A_{ij}. \tag{A11}$$

With the spin-free excitation operators, $\hat{E}_{ij} = \sum_{\sigma=\uparrow,\downarrow} a_{i\sigma}^\dagger a_{j\sigma}$ and $i \neq j$ we can observe

$$\begin{aligned}\hat{E}_{ij}\hat{E}_{ji} &= \left(\sum_\sigma a_{i\sigma}^\dagger a_{j\sigma}\right)\left(\sum_\tau a_{j\tau}^\dagger a_{i\tau}\right)\\ &= \underbrace{\sum_\sigma a_{i\sigma}^\dagger a_{j\sigma} a_{j\bar\sigma}^\dagger a_{i\bar\sigma}}_{-2A_{ij}} + \underbrace{\sum_\sigma a_{i\sigma}^\dagger a_{j\sigma} a_{j\sigma}^\dagger a_{i\sigma}}_{n_{i\sigma}(1-n_{j\sigma})}\\ &= -2A_{ij} + \sum_\sigma n_{i\sigma} - \sum_\sigma n_{i\sigma}n_{j\sigma}\\ &= -2A_{ij} + \hat{E}_{ii} - \sum_\sigma n_{i\sigma}n_{j\sigma}, \end{aligned} \tag{A12}$$

leading to the relation

$$\begin{aligned}A_{ij} &= -\frac{1}{2}\left(\hat{E}_{ij}\hat{E}_{ji} - E_{ii} + \sum_\sigma n_{i\sigma}n_{j\sigma}\right)\\ &= -\frac{1}{2}\left(\hat{e}_{ij,ji} + \sum_\sigma n_{i\sigma}n_{j\sigma}\right), \end{aligned} \tag{A13}$$

where $\hat{e}_{ij,ji} = \hat{E}_{ij}\hat{E}_{ji} - \delta_{jj}\hat{E}_{ii}$. With Eq. (A13) we can express the spin-spin interaction, Eq. (A6), as

$$\hat{\mathbf{S}}_i \cdot \hat{\mathbf{S}}_j = S_i^z \cdot S_j^z - \frac{1}{2}\left(e_{ij,ji} + \sum_\sigma n_{i\sigma}n_{j\sigma}\right). \tag{A14}$$

To express Eq. (A14) entirely in spin-free terms we can rewrite

$$\begin{aligned}\hat{S}_i^z \cdot \hat{S}_j^z - \frac{1}{2}\sum_\sigma n_{i\sigma}n_{j\sigma} &= \frac{1}{4}(n_{i\uparrow} - n_{i\downarrow})(n_{j\uparrow} - n_{j\downarrow})\\ &\quad - \frac{1}{2}(n_{i\uparrow}n_{j\uparrow} + n_{i\downarrow}n_{j\downarrow})\\ &= \frac{1}{4}(n_{i\uparrow}n_{j\uparrow} - n_{i\uparrow}n_{j\downarrow} - n_{i\downarrow}n_{j\uparrow} + n_{i\downarrow}n_{j\downarrow})\\ &\quad - \frac{1}{2}(n_{i\uparrow}n_{j\uparrow} + n_{i\downarrow}n_{j\downarrow}) \end{aligned} \tag{A15}$$

$$= -\frac{1}{4}(n_{i\uparrow}n_{j\uparrow} + n_{i\uparrow}n_{j\downarrow} + n_{i\downarrow}n_{j\uparrow} + n_{i\downarrow}n_{j\downarrow}) \tag{A16}$$

$$= -\frac{\hat{e}_{ii,jj}}{4}, \tag{A17}$$

which allows us to write the spin-spin correlation function entirely in spin-free terms as

$$\hat{\mathbf{S}}_i \cdot \hat{\mathbf{S}}_j = -\frac{1}{2}\left(\hat{e}_{ij,ji} + \frac{\hat{e}_{ii,jj}}{2}\right). \tag{A18}$$

It is worth noting that the operator $\hat{e}_{ii,jj}$ is *diagonal*, and for the Heisenberg model, with explicitly singly occupied orbitals, it is identical to one. This leads to the spin-free formulation of the Heisenberg model, (erratum to Ref. [14])

$$\begin{aligned}H &= J\sum_{\langle i,j\rangle} \hat{\mathbf{S}}_i \cdot \hat{\mathbf{S}}_j = -\frac{J}{2}\sum_{\langle i,j\rangle} \hat{e}_{ij,ji} - \frac{J}{4}\sum_{\langle i,j\rangle} 1\\ &= -\frac{J}{2}\sum_{\langle i,j\rangle} \hat{e}_{ij,ji} - \frac{JN_b}{4}, \end{aligned} \tag{A19}$$

where $\langle i,j\rangle$ indicates the summation over nearest neighbors and N_b is the number of bonds. This enables a straightforward spin-free implementation of the Heisenberg model in GUGA-FCIQMC, where only exchange-type excitations $\hat{e}_{ij,ji}$ have to be considered.

APPENDIX B: DIRAC IDENTITY

There is an alternative way to derive the spin-free Heisenberg Hamiltonian in terms unitary group generators, $\hat{E}_{ij}$, based on the Dirac identity [21,100,190]. The Dirac identity [21] is given by

$$(i,j) = \frac{1}{2} + 2\hat{\mathbf{S}}_i \cdot \hat{\mathbf{S}}_j \quad \to \hat{\mathbf{S}}_i \cdot \hat{\mathbf{S}}_j = \frac{1}{2}\left[(i,j) - \frac{1}{2}\right], \tag{B1}$$

where (i,j) indicates an exchange of electrons or spins i and j. Equation (B1) allowed Flocke and Karwowski [11] to straightforwardly express the Heisenberg Hamiltonian, Eq. (2), in terms of transpositions of spins (i,j), as

$$\hat{H} = \frac{1}{2}\sum_{ij} J_{ij}(i,j) - \frac{1}{4}\sum_{ij} J_{ij}. \tag{B2}$$

If we now use the observation by Flocke [100] that the action of the operator $(\hat{E}_{ij}\hat{E}_{ji} - \mathbb{1})$ on a "Heisenberg wave function"
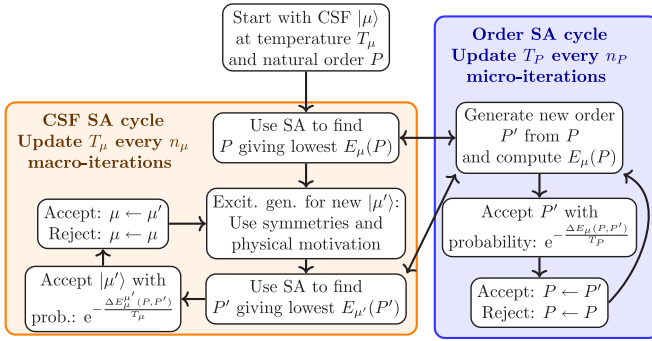
FIG. 13. Sketch of the mixed stochastic minimization procedure.

(exclusively singly occupied orbitals/spins, no empty sites) $|\phi\rangle$ is identical to a transposition

$$(\hat{E}_{ij}\hat{E}_{ji} - \mathbb{1})\,|\phi\rangle = (i,j)\,|\phi\rangle, \tag{B3}$$

and similarly that the action of $\hat{E}_{ii}$ on $|\phi\rangle$ is just the identity, $\hat{E}_{ii}\,|\phi\rangle = |\phi\rangle$, we can relate $\hat{e}_{ij,ji} = (i,j)$ and obtain the same Hamiltonian in terms of unitary group generators as in Eq. (3).

APPENDIX C: SIMULATED ANNEALING

Figure 13 shows our mixed stochastic simulated annealing (SA) approach. We start with an arbitrary CSF μ and order P, usually taken as the natural order and the corresponding highest weighted state with alternating u's and d's, $|\mu\rangle = |ududdu\ldots\rangle$, and temperature T_μ and T_P. We then use an *inner* SA loop (blue box in Fig. 13), which finds the optimal order for this CSF $|\mu\rangle$. This is done by suggesting a new order $P' \neq P$, with 2- [158,159] and 3-opt modifications [160] based on the Lin-Kernigham heuristic [161]. In the SA-spirit, this new order P' is always accepted if the diagonal matrix element, $E_\mu(P') = \langle\mu|\hat{H}(P')|\mu\rangle$ [Eq. (29)], is lower than $E(P)$, or with probability $p(P'|P) = e^{-\frac{\Delta E_\mu(P,P')}{T_P}}$, with $\Delta E_\mu(P,P') = E_\mu(P) - E_\mu(P')$. We loop over this process of suggesting new orderings P' and lower the temperature T_P every n_P micro-iterations by a user defined ratio. This is done until convergence or a set amount of micro-iterations is reached.

The final ordering P is then fed back to the main SA cycle (orange box in 13), where a new CSF $|\mu'\rangle$ is suggested stochastically. For this we use the *excitation generation* routines in the GUGA-FCIQMC method [12,13]. And for this new CSF $|\mu'\rangle$ we again use the inner loop (blue) to find the optimal ordering P' yielding the lowest $E_{\mu'}(P')$. The new state $|\mu'\rangle$ is then accepted in the macro-cycle, if its energy, $E_{\mu'}(P') = \langle\mu'|\hat{H}(P')|\mu'\rangle$, is lower than $E_\mu(P)$ or with probability $p(\mu',P'|\mu,P) = e^{-\frac{\Delta E_\mu^{\mu'}(P,P')}{T_\mu}}$, with $\Delta E_\mu^{\mu'}(P,P') =$

$E_\mu(P) - E_{\mu'}(P')$. We also loop over this macro-cycle, where the temperature T_μ is lowered every n_μ macro-iterations by a user defined ratio, and do this until convergence or a set amount of macro-iterations is reached.

For small enough systems (<30 sites), where the Hilbert space is not yet too large, we can skip the stochastic part (orange box in Fig. 13) and perform the SA to find the optimal order (blue box in Fig. 13) for every state in the Hilbert space, as this is an embarrassingly parallel task.

APPENDIX D: THE GUGA-FCIQMC METHOD

Here, we concisely summarize the main concepts of the GUGA-FCIQMC method. An in-depth description of the algorithm can be found in the literature [12,14]. The FCIQMC algorithm [131,132] is based on the imaginary-time ($\tau = it$) version of the Schrödinger equation,

$$\frac{\partial\,|\Psi(\tau)\rangle}{\partial\tau} = -\hat{H}\,|\Psi(\tau)\rangle \xrightarrow{\int d\tau}\ |\Psi(\tau)\rangle = e^{-\tau\hat{H}}\,|\Phi(0)\rangle. \tag{D1}$$

Integrating Eq. (D1) and performing a first-order Taylor expansion yields an iterable expression for the eigenstate, $|\Psi(\tau)\rangle$

$$\Psi(\tau + \Delta\tau) \approx (1 - \Delta\tau\hat{H})\Psi(\tau), \tag{D2}$$

which yields the ground state $|\Psi_0\rangle$ in the long time limit $\tau \to \infty$. In FCIQMC, the full wave function $|\Psi(\tau)\rangle$ is sampled stochastically by a set of so-called *walkers* and yields estimates for the ground- and excited-state [191] energies and properties [192] via the one- and two-body reduced density matrices [193]. More details can be found in the literature [131,132], especially in the recently published review article [13] and references therein.

In its original implementation FCIQMC is formulated in m_s-conserving SDs, and thus, does not conserve the total spin quantum number, S. For interpretability, control, and improved convergence properties, it is useful to impose the $SU(2)$ spin-rotational symmetry. We recently developed a spin-adapted implementation of FCIQMC in our laboratory [12,14,17], based on the UGA [4,5,130,133,134,136,194–196] and its graphical extension (GUGA) [124,125]. It was originally conceived for *ab initio* quantum chemical systems, but we recently applied it to study lattice models, like the two-dimensional Hubbard model [176,197,198].

The UGA is based on the spin-free formulation of quantum chemistry [129] and was pioneered by Paldus [4,7], who found an efficient usage of the Gel'fand-Tsetlin basis— a general basis for any unitary group U(n) [199–201]—to the electronic structure problem [4,5,136]. Based on this work, Shavitt developed the graphical unitary group approach (GUGA) [124–126], which provides an elegant and highly effective way to calculate Hamiltonian matrix elements between these spin-adapted basis states, also called configuration state functions (CSFs).

[1] E. Noether, Nachr. Akad. Wiss. Gött., Math.-Phys. Kl. **1918**, 235 (1918).

[2] J. J. Duistermaat and J. A. C. Kolk, *Lie Groups* (Springer, Berlin, 2000)

[3] F. Bloch, Z. Phys. **52**, 555 (1929).

[4] J. Paldus, J. Chem. Phys. **61**, 5321 (1974).

[5] J. Paldus, Phys. Rev. A **14**, 1620 (1976).

[6] J. Paldus, in *Theoretical Chemistry Advances and Perspectives*, Bd. 2, edited by H. Eyring (Elsevier Science, Amsterdam, 2012).

[7] J. Paldus, J. Math. Chem. **59**, 37 (2021).

[8] W. Pauli, Phys. Rev. **58**, 716 (1940).

[9] N. Jacobson, *Basic Algebra I: Second Edition*, Basic Algebra (Dover Publications, New York, 2009).

[10] R. Feynman and S. Weinberg, *Elementary Particles and the Laws of Physics: The 1986 Dirac Memorial Lectures* (Cambridge University Press, Cambridge, 1999).

[11] N. Flocke and J. Karwowski, Phys. Rev. B **55**, 8287 (1997).

[12] W. Dobrautz, S. D. Smart, and A. Alavi, J. Chem. Phys. **151**, 094104 (2019).

[13] K. Guther, R. J. Anderson, N. S. Blunt, N. A. Bogdanov, D. Cleland, N. Dattani, W. Dobrautz, K. Ghanem, P. Jeszenszki, N. Liebermann *et al.*, J. Chem. Phys. **153**, 034107 (2020).

[14] W. Dobrautz, Development of Full Configuration Interaction Quantum Monte Carlo Methods for Strongly Correlated Electron Systems, Ph.D. thesis, University of Stuttgart, 2019.

[15] G. Li Manni, W. Dobrautz, and A. Alavi, J. Chem. Theory Comput. **16**, 2202 (2020).

[16] G. Li Manni, W. Dobrautz, N. A. Bogdanov, K. Guther, and A. Alavi, J. Phys. Chem. A **125**, 4727 (2021).

[17] W. Dobrautz, O. Weser, N. A. Bogdanov, A. Alavi, and G. Li Manni, J. Chem. Theory Comput. **17**, 5684 (2021).

[18] G. Li Manni, Phys. Chem. Chem. Phys. **23**, 19766 (2021).

[19] W. Heisenberg, Z. Phys. **49**, 619 (1928).

[20] P. A. M. Dirac, Proc. R. Soc. A **112**, 661 (1926).

[21] P. A. M. Dirac, Proc. R. Soc. A **123**, 714 (1929).

[22] W. Heisenberg, Z. Phys. **38**, 411 (1926).

[23] J. H. Van Vleck, Phys. Rev. **45**, 405 (1934).

[24] P. Mohn, in *Magnetism in the Solid State. Solid-State Sciences* (Springer-Verlag, Berlin, 2006), Vol. 134, pp. 63–74.

[25] C. Kittel, *Quantum Theory of Solids* (Wiley, New York, 1963).

[26] W. Nolting and A. Ramakanth, *Quantum Theory of Magnetism* (Springer, Berlin, 2009).

[27] R. M. White, *Quantum Theory of Magnetism* (Springer, Berlin, 2007).

[28] A. Auerbach, *Interacting Electrons and Quantum Magnetism* (Springer, New York, 1994).

[29] P. Fazekas, *Lecture Notes on Electron Correlation and Magnetism*, Series in Modern Condensed Mat (World Scientific, Singapore, 1999).

[30] D. C. Mattis, *The Theory of Magnetism I* (Springer, Berlin, 1981).

[31] P. W. Anderson, Science **235**, 1196 (1987).

[32] S. Chakravarty, B. I. Halperin, and D. R. Nelson, Phys. Rev. B **39**, 2344 (1989).

[33] E. Manousakis, Rev. Mod. Phys. **63**, 1 (1991).

[34] E. Dagotto and T. M. Rice, Science **271**, 618 (1996).

[35] S. Eggert, I. Affleck, and M. Takahashi, Phys. Rev. Lett. **73**, 332 (1994).

[36] H. Bethe, Z. Phys. **71**, 205 (1931).

[37] M. Karabach, G. Müller, H. Gould, and J. Tobochnik, Comput. Phys. **11**, 36 (1997).

[38] L. Hulthén, Über das Austauschproblem eines Kristalles, Ph.D. thesis, Stockholm College, 1938.

[39] A. W. Sandvik, AIP Conf. Proc. **1297**, 135 (2010).

[40] U. Schollwöck, Ann. Phys. **326**, 96 (2011).

[41] D. Perez-Garcia, F. Verstraete, M. M. Wolf, and J. I. Cirac, Quantum Inf. Comput. **7**, 401 (2007).

[42] F. Verstraete, V. Murg, and J. Cirac, Adv. Phys. **57**, 143 (2008).

[43] S. Östlund and S. Rommer, Phys. Rev. Lett. **75**, 3537 (1995).

[44] S. R. White, Phys. Rev. Lett. **69**, 2863 (1992).

[45] S. R. White, Phys. Rev. B **48**, 10345 (1993).

[46] U. Schollwöck, Rev. Mod. Phys. **77**, 259 (2005).

[47] P. Pippan, S. R. White, and H. G. Evertz, Phys. Rev. B **81**, 081103(R) (2010).

[48] D. Dey, D. Maiti, and M. Kumar, Pap. Phys. **8**, 080006(2016).

[49] M. Srednicki, Phys. Rev. Lett. **71**, 666 (1993).

[50] G. Vidal, J. I. Latorre, E. Rico, and A. Kitaev, Phys. Rev. Lett. **90**, 227902 (2003).

[51] M. B. Hastings, J. Stat. Mech: Theory Exp. (2007) P08024.

[52] G. Vidal, Phys. Rev. Lett. **99**, 220405 (2007).

[53] V. Murg, F. Verstraete, and J. I. Cirac, Phys. Rev. B **79**, 195119 (2009).

[54] R. Orús, Ann. Phys. **349**, 117 (2014).

[55] L. Wang, Z.-C. Gu, F. Verstraete, and X.-G. Wen, Phys. Rev. B **94**, 075143 (2016).

[56] S.-H. Li, Q.-Q. Shi, Y.-H. Su, J.-H. Liu, Y.-W. Dai, and H.-Q. Zhou, Phys. Rev. B **86**, 064401 (2012).

[57] K. Binder, ed., *Applications of the Monte Carlo Method in Statistical Physics* (Springer, Berlin, 1984).

[58] E. Y. Loh, J. E. Gubernatis, R. T. Scalettar, S. R. White, D. J. Scalapino, and R. L. Sugar, Phys. Rev. B **41**, 9301 (1990).

[59] M. Troyer and U.-J. Wiese, Phys. Rev. Lett. **94**, 170201 (2005).

[60] D. H. Lee, J. D. Joannopoulos, and J. W. Negele, Phys. Rev. B **30**, 1599 (1984).

[61] M. Suzuki, Commun. Math. Phys. **51**, 183 (1976).

[62] M. Suzuki, Prog. Theor. Phys. **56**, 1454 (1976).

[63] H. F. Trotter, Proc. Am. Math. Soc. **10**, 545 (1959).

[64] M. Nyfeler, F.-J. Jiang, F. Kämpfer, and U.-J. Wiese, Phys. Rev. Lett. **100**, 247206 (2008).

[65] A. W. Sandvik, in *Springer Proceedings in Physics* (Springer, Berlin, 2002), pp. 182–187.

[66] A. W. Sandvik and J. Kurkijärvi, Phys. Rev. B **43**, 5950 (1991).

[67] O. F. Syljuåsen and A. W. Sandvik, Phys. Rev. E **66**, 046701 (2002).

[68] A. W. Sandvik, Phys. Rev. B **59**, R14157 (1999).

[69] J. Gubernatis, N. Kawashima, and P. Werner, *Quantum Monte Carlo Methods* (Cambridge University Press, Cambridge, 2016).

[70] N. V. Prokof'ev, B. V. Svistunov, and I. S. Tupitsyn, J. Exp. Theor. Phys. **87**, 310 (1998).

[71] R. Blankenbecler, D. J. Scalapino, and R. L. Sugar, Phys. Rev. D **24**, 2278 (1981).

[72] J. E. Hirsch, Phys. Rev. B **31**, 4403 (1985).

[73] H. G. Evertz, G. Lana, and M. Marcu, Phys. Rev. Lett. **70**, 875 (1993).

[74] H. G. Evertz, Adv. Phys. **52**, 1 (2003).

[75] M. H. Kalos, D. Levesque, and L. Verlet, Phys. Rev. A **9**, 2178 (1974).

[76] D. M. Ceperley, Rev. Mod. Phys. **67**, 279 (1995).

[77] S. Zhang and H. Krakauer, Phys. Rev. Lett. **90**, 136401 (2003).

[78] K. Ghanem, N. Liebermann, and A. Alavi, Phys. Rev. B **103**, 155135 (2021).

[79] S. Sorella, S. Baroni, R. Car, and M. Parrinello, Europhys. Lett. **8**, 663 (1989).

[80] J. E. Hirsch and R. M. Fye, Phys. Rev. Lett. **56**, 2521 (1986).

[81] F. Assaad and H. Evertz, in *Computational Many-Particle Physics* (Springer, Berlin, 2008), pp. 277–356.

[82] M. Troyer, M. Imada, and K. Ueda, J. Phys. Soc. Jpn. **66**, 2957 (1997).

[83] B. B. Beard and U.-J. Wiese, Phys. Rev. Lett. **77**, 5130 (1996).

[84] W. M. C. Foulkes, L. Mitas, R. J. Needs, and G. Rajagopal, Rev. Mod. Phys. **73**, 33 (2001).

[85] D. Tahara and M. Imada, J. Phys. Soc. Jpn. **77**, 114701 (2008).

[86] G. Carleo and M. Troyer, Science **355**, 602 (2017).

[87] R. G. Melko, G. Carleo, J. Carrasquilla, and J. I. Cirac, Nat. Phys. **15**, 887 (2019).

[88] Y. Nomura, A. S. Darmawan, Y. Yamaji, and M. Imada, Phys. Rev. B **96**, 205152 (2017).

[89] L. Yang, Z. Leng, G. Yu, A. Patel, W.-J. Hu, and H. Pu, Phys. Rev. Research **2**, 012039(R) (2020).

[90] K. Choo, G. Carleo, N. Regnault, and T. Neupert, Phys. Rev. Lett. **121**, 167204 (2018).

[91] A. Nagy and V. Savona, Phys. Rev. Lett. **122**, 250501 (2019).

[92] K. Choo, T. Neupert, and G. Carleo, Phys. Rev. B **100**, 125124 (2019).

[93] X. Liang, W.-Y. Liu, P.-Z. Lin, G.-C. Guo, Y.-S. Zhang, and L. He, Phys. Rev. B **98**, 104426 (2018).

[94] J. Chen, S. Cheng, H. Xie, L. Wang, and T. Xiang, Phys. Rev. B **97**, 085104 (2018).

[95] I. Glasser, N. Pancotti, M. August, I. D. Rodriguez, and J. I. Cirac, Phys. Rev. X **8**, 011006 (2018).

[96] D.-L. Deng, X. Li, and S. Das Sarma, Phys. Rev. X **7**, 021021 (2017).

[97] N. Flocke, Phys. Rev. B **56**, 13673 (1997).

[98] J. Karwowski, J. Math. Chem. **23**, 127 (1998).

[99] J. Karwowski and N. Flocke, Int. J. Quantum Chem. **90**, 1091 (2002).

[100] N. Flocke and J. Karwowski, in *Theoretical and Computational Chemistry* (Elsevier, Amsterdam, 2002), pp. 603–634.

[101] N. Flocke, Comput. Phys. Commun. **106**, 114 (1997).

[102] W. Duch and J. Karwowski, Int. J. Quantum Chem. **22**, 783 (1982).

[103] K. Ruedenberg, Phys. Rev. Lett. **27**, 1105 (1971).

[104] W. Duch and J. Karwowski, Comput. Phys. Rep. **2**, 93 (1985).

[105] R. Pauncz, *Spin Eigenfunctions: Construction and Use* (Springer, Berlin, 1979).

[106] R. Pauncz, *The Symmetric Group in Quantum Chemistry* (CRC Press, Boca Raton, FL, 2018).

[107] S. Sharma and G. K.-L. Chan, J. Chem. Phys. **136**, 124121 (2012).

[108] I. P. McCulloch and M. Gulácsi, Europhys. Lett. **57**, 852 (2002).

[109] S. Wouters, W. Poelmans, P. W. Ayers, and D. V. Neck, Comput. Phys. Commun. **185**, 1501 (2014).

[110] T. Xiang, J. Lou, and Z. Su, Phys. Rev. B **64**, 104414 (2001).

[111] W. Tatsuaki, Phys. Rev. E **61**, 3199 (2000).

[112] P. Nataf and F. Mila, Phys. Rev. B **97**, 134420 (2018).

[113] S. Singh and G. Vidal, Phys. Rev. B **86**, 195114 (2012).

[114] A. Fledderjohann, A. Klümper, and K.-H. Mütter, J. Phys. A: Math. Theor. **44**, 475302 (2011).

[115] S. Singh, H.-Q. Zhou, and G. Vidal, New J. Phys. **12**, 033029 (2010).

[116] G. Sierra and T. Nishino, Nucl. Phys. B **495**, 505 (1997).

[117] T. Wada and T. Nishino, Comput. Phys. Commun. **142**, 164 (2001).

[118] E. Shpagina, F. Uskov, N. Il'in, and O. Lychkovskiy, J. Phys. A: Math. Theor. **53**, 075301 (2020).

[119] F. Uskov and O. Lychkovskiy, J. Phys.: Conf. Ser. **1163**, 012057 (2019).

[120] I. G. Bostrem, A. S. Ovchinnikov, and V. E. Sinitsyn, Theor. Math. Phys. **149**, 1527 (2006).

[121] T. Heitmann and J. Schnack, Phys. Rev. B **99**, 134405 (2019).

[122] I. G. Bostrem, A. S. Ovchinnikov, and V. E. Sinitsyn, Symmetry **2**, 722 (2010).

[123] V. E. Sinitsyn, I. G. Bostrem, and A. S. Ovchinnikov, J. Phys. A: Math. Theor. **40**, 645 (2007).

[124] I. Shavitt, Int. J. Quantum Chem. **12**, 131 (1977).

[125] I. Shavitt, Int. J. Quantum Chem. **14**, 5 (1978).

[126] I. Shavitt, in *The Unitary Group for the Evaluation of Electronic Energy Matrix Elements*, edited by J. Hinze (Springer, Berlin, 1981), pp. 51–99.

[127] J. Paldus and M. J. Boyle, Phys. Scr. **21**, 295 (1980).

[128] J. Paldus, in *Unitary Group Approach to Many-Electron Correlation Problem*, edited by J. Hinze (Springer, Berlin, 1981), pp. 1–50.

[129] F. Matsen, in *Advances in Quantum Chemistry* (Elsevier, Amsterdam, 1964), pp. 59–114.

[130] F. A. Matsen, Int. J. Quantum Chem. **8**, 379 (1974).

[131] G. H. Booth, A. J. W. Thom, and A. Alavi, J. Chem. Phys. **131**, 054106 (2009).

[132] D. Cleland, G. H. Booth, and A. Alavi, J. Chem. Phys. **132**, 041103 (2010).

[133] B. R. Brooks and H. F. Schaefer, J. Chem. Phys. **70**, 5092 (1979).

[134] B. R. Brooks, W. D. Laidig, P. Saxe, N. C. Handy, and H. F. Schaefer III, Phys. Scr. **21**, 312 (1980).

[135] F. Matsen, in *Advances in Quantum Chemistry* (Elsevier, Amsterdam, 1978), Vol. 11, pp. 223–250.

[136] J. Paldus, in *Electrons in Finite and Infinite Structures* (Springer, New York, 1977), pp. 411–429.

[137] T. Helgaker, P. Jørgensen, and J. Olsen, *Molecular Electronic-Structure Theory* (John Wiley & Sons, Chichester, 2000).

[138] E. Wigner, *Gruppentheorie und ihre Anwendung auf die Quantenmechanik der Atomspektren* (Vieweg + Teubner Verlag, Wiesbaden, Germany, 1931).

[139] W. I. Salmon, in *Advances in Quantum Chemistry* (Elsevier, Amsterdam, 1974), Vol. 8, pp. 37–94.

[140] W. G. Harter and C. W. Patterson, *A Unitary Calculus for Electronic Orbitals* (Springer-Verlag, Berlin, 1976).

[141] See Supplemental Material at http://link.aps.org/supplemental/10.1103/PhysRevB.105.195123 for computational details, examples of expansion of CSFs in terms of SDs, reference weight and orderings for a 4×2 Heisenberg ladder and sample input files for BLOCK DMRG, NECI FCIQMC and the LKH TSP calculations (2021).

[142] M. E. Fisher, Rev. Mod. Phys. **46**, 597 (1974).

[143] R. Hoffmann and J.-P. Malrieu, Angew. Chem. Int. Ed. **59**, 13694 (2020).

[144] J.-P. Malrieu and N. Guihéry, Phys. Rev. B **63**, 085110 (2001).

[145] K. G. Wilson, Rev. Mod. Phys. **47**, 773 (1975).

[146] L. P. Kadanoff, Phys. Phys. Fiz. **2**, 263 (1966).

[147] D. L. Applegate, R. E. Bixby, V. Chvatál, and W. J. Cook, *The Traveling Salesman Problem: A Computational Study* (Princeton University Press, Princeton, 2006).

[148] C. H. Papadimitriou and K. Steiglitz, *Combinatorial Optimization: Algorithms and Complexity* (Dover Publishing, New York, 1998).

[149] G. Dantzig, *Linear Programming and Extensions* (RAND Corporation, Santa Monica, 1963).

[150] C. E. Miller, A. W. Tucker, and R. A. Zemlin, JACM **7**, 326 (1960).

[151] G. Dantzig, R. Fulkerson, and S. Johnson, J. Oper. Res. Soc. Am. **2**, 393 (1954).

[152] T. C. Koopmans and M. Beckmann, Econometrica **25**, 53 (1957).

[153] A. Khachaturyan, S. Semenovsovskaya, and B. Vainshtein, Acta Cryst. A **37**, 742 (1981).

[154] P. J. M. van Laarhoven and E. H. L. Aarts, *Simulated Annealing: Theory and Applications* (Springer, Netherlands, 1987).

[155] S. Kirkpatrick Jr., C. D. Gelatt, and M. P. Vecchi, Science **220**, 671 (1983).

[156] V. Černý, J. Optim. Theory Appl. **45**, 41 (1985).

[157] M. Pincus, Oper. Res. **18**, 1225 (1970).

[158] G. A. Croes, Oper. Res. **6**, 791 (1958).

[159] M. M. Flood, Oper. Res. **4**, 61 (1956).

[160] S. Lin, Bell Syst. Tech. J. **44**, 2245 (1965).

[161] S. Lin and B. W. Kernighan, Oper. Res. **21**, 498 (1973).

[162] K. Helsgaun, Eur. J. Oper. Res. **126**, 106 (2000).

[163] K. Helsgaun, Math. Prog. Comp. **1**, 119 (2009).

[164] J. Olsen, J. Chem. Phys. **141**, 034112 (2014).

[165] B. S. Fales and T. J. Martínez, J. Chem. Phys. **152**, 164111 (2020).

[166] M. Kawamura, K. Yoshimi, T. Misawa, Y. Yamaji, S. Todo, and N. Kawashima, Comput. Phys. Commun. **217**, 180 (2017).

[167] J. Sato, M. Shiroishi, and M. Takahashi, Nucl. Phys. B **729**, 441 (2005).

[168] L. Wang and S. G. Chung, J. Phys. Soc. Jpn. **81**, 114712 (2012).

[169] T. Hikihara and A. Furusaki, Phys. Rev. B **69**, 064427 (2004).

[170] A. Lüscher and A. M. Läuchli, Phys. Rev. B **79**, 195102 (2009).

[171] A. M. Läuchli, J. Sudan, and R. Moessner, Phys. Rev. B **100**, 155142 (2019).

[172] M. Karbach, K. Hu, and G. Müller, Comput. Phys. **12**, 565 (1998).

[173] G. K.-L. Chan and M. Head-Gordon, J. Chem. Phys. **116**, 4462 (2002).

[174] D. Ghosh, J. Hachmann, T. Yanai, and G. K.-L. Chan, J. Chem. Phys. **128**, 144117 (2008).

[175] R. Olivares-Amaya, W. Hu, N. Nakatani, S. Sharma, J. Yang, and G. K.-L. Chan, J. Chem. Phys. **142**, 034102 (2015).

[176] S. Yun, W. Dobrautz, H. Luo, and A. Alavi, Phys. Rev. B **104**, 235102 (2021).

[177] M. Motta, D. M. Ceperley, G. K.-L. Chan, J. A. Gomez, E. Gull, S. Guo, C. A. Jiménez-Hoyos, T. N. Lan, J. Li, F. Ma, A. J. Millis, N. V. Prokof'ev, U. Ray, G. E. Scuseria, S. Sorella, E. M. Stoudenmire, Q. Sun, I. S. Tupitsyn, S. R. White, D. Zgid, and S. Zhang (Simons Collaboration on the Many-Electron Problem), Phys. Rev. X **7**, 031059 (2017).

[178] M. Motta, C. Genovese, F. Ma, Z.-H. Cui, R. Sawaya, G. K.-L. Chan, N. Chepiga, P. Helms, C. Jiménez-Hoyos, A. J. Millis, U. Ray, E. Ronca, H. Shi, S. Sorella, E. M. Stoudenmire, S. R. White, and S. Zhang (Simons Collaboration on the Many-Electron Problem), Phys. Rev. X **10**, 031058 (2020).

[179] M. Ali, arXiv:2103.01111.

[180] O. Legeza and J. Sólyom, Phys. Rev. B **68**, 195116 (2003).

[181] G. Moritz, B. A. Hess, and M. Reiher, J. Chem. Phys. **122**, 024107 (2005).

[182] J. Rissler, R. M. Noack, and S. R. White, Chem. Phys. **323**, 519 (2006).

[183] G. Barcza, O. Legeza, K. H. Marti, and M. Reiher, Phys. Rev. A **83**, 012508 (2011).

[184] A. O. Mitrushchenkov, G. Fano, R. Linguerri, and P. Palmieri, Int. J. Quantum Chem. **112**, 1606 (2012).

[185] S. F. Keller and M. Reiher, CHIMIA **68**, 200 (2014).

[186] M. Fiedler, Czech. Math. J. **23**, 298 (1973).

[187] M. Fiedler, Czech. Math. J. **25**, 607 (1975).

[188] M. Juvan and B. Mohar, Discrete Appl. Math. **36**, 153 (1992).

[189] W. Pauli, Z. Phys. **31**, 765 (1925).

[190] J. Katriel, J. Paldus, and R. Pauncz, Int. J. Quantum Chem. **28**, 181 (1985).

[191] N. S. Blunt, S. D. Smart, G. H. Booth, and A. Alavi, J. Chem. Phys. **143**, 134117 (2015).

[192] N. S. Blunt, G. H. Booth, and A. Alavi, J. Chem. Phys. **146**, 244105 (2017).

[193] C. Overy, G. H. Booth, N. S. Blunt, J. J. Shepherd, D. Cleland, and A. Alavi, J. Chem. Phys. **141**, 244117 (2014).

[194] J. Paldus, Int. J. Quantum Chem. **9**, 165 (1975).

[195] L. C. Biedenharn, J. Math. Phys. **4**, 436 (1963).

[196] M. J. Downward and M. A. Robb, Theor. Chim. Acta **46**, 129 (1977).

[197] K. Guther, W. Dobrautz, O. Gunnarsson, and A. Alavi, Phys. Rev. Lett. **121**, 056401 (2018).

[198] W. Dobrautz, H. Luo, and A. Alavi, Phys. Rev. B **99**, 075119 (2019).

[199] I. M. Gel'fand and M. L. Cetlin, Doklady Akad. Nauk SSSR (N.S.) **71**, 825 (1950).

[200] I. M. Gel'fand and M. L. Cetlin, Doklady Akad. Nauk SSSR (N.S.) **71**, 1017 (1950), Am. Math. Soc. Transl. **64**, 116 (1967).

[201] I. M. Gel'fand, Mat. Sb. (N.S.) **26**, 103 (1950).